Understanding the equilibrium behaviour of a novel phase splitting solvent in the presence of high pressure CO_2

Arjen Kingma
Master Thesis combined with an internship at TNO
Energy Science master
Utrecht University
The Netherlands

TNO innovation for life

Acknowledgement:

This thesis is the result of an 30 ECTS internship at TNO's Gas Treatment department which was conducted between November 2014 and June 2015. During this period, I spent a lot of time in the laboratory working on experimental set-ups and analysing samples with apparatus I had never seen before. A number of people have helped me getting acquainted with the equipment and I would like to use this opportunity to thank (in no particular order) Daphne Bakker, Henk Trap, Rebecca Leenman and Arjen Huizinga for their help.

Furthermore I would like to thank my supervisors for their support and help, without which conducting this research and writing this thesis would have taken much more time. Even though Earl Goetheer was not one of my supervisors I would like to thank him here as well for all the support he has given.

Arjen Kingma
20th of June, 2015

Author:
ing. Arjen Kingma

Supervision:

TNO:
Purvil Khakharia - purvil.khakharia@tno.nl

Utrecht Univeristy:
Ir. Mijndert van der Spek - M.W.vanderSpek@uu.nl
Dr. Ir. Andrea Ramirez - C.a.ramirez@uu.nl

Cover picture: the Bab Sour Gas Treatment Facility in the United Arab Emirates, jointly developed by Royal Dutch Shell and the Abu Dhabi National Oil Company. The plant is designed to process ca. 28 million m^3 of natural gas per day coming from the Bab gas field, which contains ca. 50 % CO_2 and 15 % H_2S (1).

Abstract

The main objective of this research was to increase the knowledge of carbon capture solvents which form two phases when absorbing high pressure CO_2, e.g. from natural gas fields. Based on the results of previous experiments, a literature study and already existing knowledge of carbon capture, a number of possible blends have been identified. During the screening experiments, the MAC was used to rapidly determine whether or not a blend forms two phases or not. The results indicate that besides water sulfolane, MDEA and a primary/secondary amine have to be present for the two phases to form. However, too little information is available to draw any solid conclusions.

After the screening experiments, high pressure test were conducted in the VLE to determine the loading and phase composition at various partial pressures. At random pressure intervals, samples were taken of either phase, which were analysed for e.g. composition and loading. The tested blend consisted of 10 wt% AEP, 25 wt% water, 30% MDEA and 35 wt% sulfolane. It was observed that the heavy (or physical) phase is predominantly sulfolane (>85 wt%), with small amounts of water and MDEA. Meanwhile, the light (or chemical) phase consists of all four components being present with fractions between 11 and 35 wt%. At a CO_2 partial pressure of 1.500 kPa, over 4,1 mole of CO_2 can be absorbed per litre of blend. The chemical (top) phase absorbed the majority of the CO_2 (4,5 mole/L), while the physical (bottom) phase has a loading of ca. 1,56 mole/L.

Heating the chemical phase to 120 ^{0}C causes the majority of the absorbed CO_2 to be stripped, as at 20 kPa the loading reduces to 0,16 mole L^{-1}. Hence, the chemical phase has a cyclic loading of ca. 3,84 mole L^{-1}; assuming a 700 kPa CO_2 partial pressure and 30 kPa partial pressure in the stripper. The physical phase has – again 700 kPa – a cyclic loading of ca. 0,62 mole L^{-1}. Combining these loadings gives a cyclic loadings of 3,19 mole L^{-1}, which is a 10 % increase compared to an aMDEA blend being used at the same conditions.

Furthermore, the energy associated with this process is ca. 55 % less, compared to the aMDEA process, which implies that a significant reduction in energy consumption can be achieved. However, it should be noted that this statement is based on VLE figures which are at the limit of the apparatus; which means that some deviation might have been caused by this.

Also, the equipment which was used to determine the phase composition at various partial pressures (i.e. the GC and Karl Fischer titrations) proved to be unreliable. The sulfolane concentration in the physical phase and the water content of either of the phases could – for unknown reasons – not be determined accurately

Ultimately, the result of this thesis is that more is known about the composition of the two phases when CO2 is absorbed at high pressure and some estimates are made for the (energetic) performances of the blend. The knowledge of this blend can be further expanded by future research, focussing not only on improving the analytical methods used but also optimizing the blend.

Table of contents

1 Introduction

As the world's energy demand continues to grow, the demand for natural gas has been increasing accordingly (2). Estimates are that by 2050 the demand for natural gas will have doubled – based on the 2005 consumption (3). The French oil company Total estimates that 40% of the proven gas reserves contain acid gas components, roughly equal to 73 trillion m^3 of natural gas (4); equal to the global natural gas consumption for some 23 years (2010 consumption figures) (5). Other estimates are even higher, suggesting that 50 % of the known gas reserves contain more than 2 % CO_2 (6).

These numbers illustrate that there is a huge amount of natural gas available, if the acid components can be removed. Having removed the acid components enables to use lower grade steel in terms of resistance to corrosion, using smaller equipment and avoiding (toxic) CO_2 and H_2S emissions (7). The removed gasses can be released into the atmosphere; even though these can also be used to increase production via a technique called enhanced oil or gas production (8) or fed to a Claus unit (9). However, due to the separation techniques and sizes of the equipment can acid gas removal be costly in terms of both capital and energy. The acid gas removal facility can cost over 50% of the total CAPEX involved when developing a new field (10) while requiring ca. 8 MW per mole % CO_2 removed (11).

Up to date, there are a number of techniques which can be used to upgrade the natural gas, such as absorption, membrane separation, chemical adsorption and cryogenic distillation (12). Which technology is used depends on many variables such as the natural gas flow, the required purity, the access to electricity, the availability of a Claus unit besides the preferences the operator might have.

When choosing for absorption, either chemical or physical absorption can be used. Chemical absorption involves an acid-base reaction (12) between the (often amine based) solvent and the sour gasses whereas physical absorption is based on the gas dissolving into the solvent (9). As a result, chemical absorption is often used when partial pressures are moderate (12) or when stringent requirements are in place (e.g. for LNG or transport via pipelines) (13). Physical absorption becomes attractive at partial pressures roughly above 700 kPa, as higher pressures enable more CO_2 to dissolve in the physical solvent (12). However, a lower purity can be obtained when using physical absorption.

As a chemical bond is formed during absorption, this has to be broken during regeneration of the solvent. As absorption is an exothermic process (14), it usually takes place at ca. 40 ^{0}C (15) (16); the energy released is often referred to as the heat of absorption. As a result, the reverse reaction (stripping) is endothermic. As a result, strippers are typically operated at about 120 ^{0}C (14) (17); and – as a result – consume a lot of energy. Since no chemical bond is formed during physical absorption, regeneration can often be achieved by reducing the pressure in e.g. a flash drum (9) (18). As a result, regeneration of a physical solvent usually requires less energy than regeneration of a chemical solvent (12).

The large amount of energy required during regeneration is one of the major drawbacks when using amines for gas treatment, besides the thermal degrading of amines and relatively low loading (mole CO_2 per mole amine) (19) (20). Hence, there has been a constant quest for improved solvents. As a result, currently used solvents include monoethanolamine (13), methyldiethanolamine, piperazine and 2-amino-2-methyl-1-propanol (21) and aminoethylpiperazine (22).

The 1990's saw the introduction of amine blends in attempts to overcome most of the disadvantages associated with amine based solvents (9). By mixing primary and tertiary amines it is attempted to increase the loading and rate of absorption (23) (24), reduce the amount of solvent required, lower the regeneration energy and/or to reduce the thermal degradation of amines during operation (25).

An interesting phenomena is that certain blends which have recently been developed form two liquid phases when CO_2 is absorbed. One phase contains most of the CO_2, whereas the other phase hardly contains any. As a result, only the rich phase has to be stripped while the lean phase can directly be fed to the absorber. Hence, less solvent has to be stripped and thus less energy is required (26) (27) (28).

This development raised the question whether it is possible to develop a blend specifically aimed for treating natural gas. This implies absorption at high partial pressures, as gas treatment plants operate at pressures up to 4 MPa (29).

Figure 1 - Previous TNO experiments showing the unloaded (L) and loaded (R) blend. The loaded blend clearly shows that two distinct phases have been formed, as can be seen from the colour difference.

Figure 1 (i.e. the reference experiment) shows the starting point of TNO's Bulk CO_2 removal project. It shows two reactors containing the same solvent. The left photo shows the blend before absorbing CO_2 while the right picture shows the blend having absorbed CO_2 at a maximum pressure of 550 kPa.

The results shown in Figure 1 sparked the idea that such a blend (a mixture of physical and chemical solvents which form two phases when absorbing high pressure CO_2) can be used for high pressure applications. Using a blend of chemical and physical absorbance has a number of (theoretical) advantages: 1) the regeneration energy is less thanks due to the physical solvent absorbing the majority of the CO_2; 2) high purity levels can be reached thanks to the chemical absorption and 3) the costs can reduce as the plant size can be reduced.

1.1 Main objective

This thesis is part of the bulk removal project and aims at *1) understanding the equilibrium behaviour and 2) estimating the energy consumption of a novel phase splitting solvent in the presence of high pressure CO_2*[1].

1.2 Sub questions and approach

In order to fore fill this thesis´s main objective, a number of sub objectives have been formulated:

- Determine criteria for the phase split to occur;
- Design and conduct an experiment which allows to determine important parameters at high pressure;
- Estimate the energy consumption during carbon capture.

This includes designing an experimental set-up which allows for measuring the indicated parameters at various pressures. Furthermore, a back of envelope calculations will be used for a techno economic analysis to estimate if this technology is competitive with conventional techniques.

[1] For simplicity and safety reasons, only CO_2 will be considered. Other sour gasses such as H_2S lie therefore beyond the scope of this thesis.

2 Literature study

The starting point of this thesis is an experiment conducted in the spring of 2014. When testing various carbon capture blends, it was noticed that some of the solvents formed two phases when absorbing CO_2 under high pressure; see Figure 1. Analysis of the phases showed that the top phase contained most of the water and the chemical solvents while the bottom phase contained mainly the physical solvent and trace amounts of water while. This chapter aims to summarizes the available data about CO_2 capture solvents and experimental techniques which are used. Both at high and low pressure results are displayed as there is little information available about high pressure capture.

2.1 Chemical solvents

Much of the solvents used for chemical absorption are based on amines, which can be divided into three types: primary, secondary and tertiary amines. The division is based on the number of functional groups (e.g. alcohols or alkyl groups) bonded to the nitrogen atom. As primary and secondary amines both have at least one hydrogen bonded to the nitrogen atom, their reaction mechanism in the same (19) (30). For that reason, 'primary amine' will be used to refer to both primary and secondary amines, unless it is otherwise indicated. Since tertiary amines have three functional groups and thus cannot accommodate an additional hydrogen, CO_2 is absorbed via a different mechanism (30).

2.1.1 Primary & secondary amines

Primary amines are amines in one functional group (R^1) is bound to the nitrogen atom (see figure Figure 2); the other two atoms being hydrogen. The fundamental difference with secondary amines is that instead of one, two functional groups (R^1 and R^2) are bonded to the nitrogen atom(see Figure 3). This functional group can be any functional group; even though they are often based on an alcohol as an alcohol reduces the vapour pressure and increases the solubility of the amine in water (26).

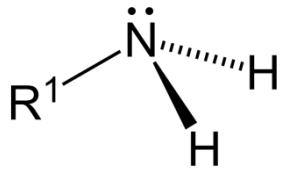

Figure 2 - Primary amine (31)

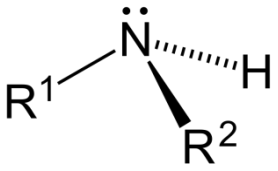

Figure 3 - Secondary amine (32)

The reaction of absorbing the CO_2 can be described with the following overall reaction:

$$CO_2 + 2\,RNH_2 \leftrightarrow RNHCOO^- + RNH^+ \quad (30)$$

As can be seen from the reaction, two mole of amine are required in order to absorb one mole of CO_2. As a result, primary amines can have a maximum loading of 0,5 mole of CO_2 per mole amine, which is less than the capacity of tertiary amines (30) (33); see also the next paragraph. However, a major advantage of primary amines – compared to tertiary amines – is that that the carbamate ($RNHCOO^-$) is formed rapidly and that the absorption reaction is relatively fast (19).

2.1.2 Tertiary amines

Tertiary amines differ from primary amines in that the nitrogen atom is bound to three functional groups, instead of one or two for the primary or secondary amines. See also Figure 4.

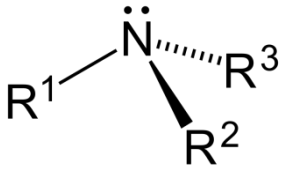

Figure 4 - Tertiary amine (34)

A consequence, there is no hydrogen atom bonded to the central nitrogen to accommodate the carbamate formation. Hence, the reaction to absorb CO_2 is different:

$$CO_2 + RR_1R_2N + H_2O \leftrightarrow HCO_3^- + RR_1R_2NH^+ \quad (30)$$

Instead of hydrogen, water is being used in the reaction. Thus, water has to be present for tertiary amines to dissolve any CO_2; a pure tertiary amine won't dissolve any CO_2. Also, the maximum loading of a tertiary amine is higher compared to primary amines. Per mole of amines one mole of CO_2 can be absorbed (30), making the theoretical loading is twice as high (1 mole CO_2 per mole amine). The downside of this improved loading is that the reaction rate is smaller (16).

2.1.3 Amine blends

In an attempt to combine the best of both – high absorption rates from the primary amines with high loadings of the tertiary amines (15) – a number of blends have been developed; all of which are operated close to atmospheric pressures: the HySWEET solvent (Total oil company) (4); the DMX mixture (French Institute of Petroleum) (26); diethylethanolamine (DEEA) combined with n-methyl-1,3-diaminopropane (MAPA) (Norwegian University of Science and Technology) (27), activated MDEA which consists of methyldiethanolamine (MDEA) combined with piperazine (Pz) and is developed by BASF (35) and TBS-3, a mixture of n,n-dimethylcyclohexamine [DMCA], n-methylcyclohexylamine [MCA] and AMP (jointly developed by Imperial College London and the Technical University of Dortmund) (28).

According to all authors, their mixtures are a major improvement in terms of energy consumption compared to various benchmark technologies. According to Liebental et al., the heat requirements of the reboiler can be reduced with over 30 % when comparing the DEEA/MAPA mixture with a 30 wt% MEA solution (27). Also, the TBS-3 mixture is said to have a loading which is at least 150 % higher (compared to a 30 wt% MEA solution) while being able to regenerate at 80 ^{0}C (28). Unfortunately, units missing in the presented graphs (4) or not clearly stating which blend has been used (26) makes comparison/confirmation of the results and claims troublesome.

2.2 Physical solvents

The main difference between chemical and physical absorption is that physical solvents do not chemically react when absorbing the CO_2. Instead, the CO_2 dissolves into the liquid; the amount of which can be approximated by using Henry's Law (14) (36) (37). Strictly speaking can Henry's Law only be for ideal gasses at low pressures, even though the expression is also used for describing the behaviour of high pressure physical solvents (38).

Henry's Law states that the amount of gas dissolved into a liquid is directly proportional to the partial pressure. Hence – given an infinite partial pressure – an infinite amount of gas can be dissolved/absorbed in a certain liquid. However, given that most applications have a maximum partial CO_2 pressure, there is a maximum of how much gas can be physically absorbed. Mathematically, this can be represented as

$$P = K_h \cdot c$$

with:
P = partial pressure
K_h = Henry constant

C = concentration

This formula explains why flashing is used to regeneration the solvent: flashing reduces the pressure during which the partial pressure is also reduced. Hence there is a force which drives the gas out of the solvent via which the solvent is regenerated.

As a result, there are no functional groups required for physical solvents; which implies that almost all liquids can be used as such. However, high loadings are clearly desired, as these reduce the solvent circulation rate. Also, valuable components of the treated gas (e.g. methane and hydrogen) should – for obvious reasons – not significantly dissolve in the solvent. Furthermore, the solvent should be non-corrosive, non-reactive, have a low vapour pressure and be available at reasonable costs (note that these criteria also apply for chemical solvents). Hence, only a limited number of physical solvents currently being used (9).

2.3 Selection criteria for solvents or blends

The cyclic capacity of the novel solvent is often cited as one of the prime factors during the selecting stages of a novel solvent. This is the result of the cyclic capacity significantly influencing the overall size and energetic performances of the capture plant (39) (40).

However, there are also other criteria which are used to select (or reject) a possible novel solvent or blend: the heat and rate of absorption (i.e. how fast is CO_2 absorbed by the solvent and how much energy is required during regeneration of the solvent) and the extent to which amines tend to degrade during normal operations. Table 1 shows a number of criteria which are frequently used:

Table 1 – Criteria for selecting novel solvents and reference to sources in which these have been used

Criteria	Unit	Reference
(cyclic) CO_2 loading	Mole CO_2 (mole amine)$^{-1}$ or mole L^{-1}	(40) (41) (42) (43) (44)
Rate of absorption	Mole CO_2 L^{-1} s^{-1}	(20) (45)
Heat of absorption	kJ per mole CO_2	(42) (45)
Amine degradation	Gr (gr solvent)$^{-1}$ s^{-1}	(12) (35)
Regeneration energy	GJ (ton CO_2)$^{-1}$	(43) (46)
Solvent viscosity	cP	(18) (22) (30)

2.4 Commonly used solvent screening experiments

In the previous paragraph, a number of frequently used selecting criteria have been described. This paragraph continues with describing experiments which are often used to determine these characteristics.

Many of the used apparatus are designed to determine the loading at various CO_2 partial pressures to be construct a loading curve (partial pressure vs. loading). These curves are valuable, as these curves are generally used to predict the loading at various pressures. Hence, these graphs are often published, as can be seen in e.g. Ma'mum et al. (20), Murrita-Guevara et al. (47) and Monteiro et al. (25).

Many researches use a continuously flow of CO_2 during their experiments (20) (40), in which pulses of CO_2 are injected into the solvent containing vessels. An advantage of a continuous flow is that other parameters (e.g. on reaction kinetics) can be obtained during the same experiment. For example, Figure 5 shows an experimental set-up which is used to determine the reaction kinetics and loading of a solvent simultaneously. However, many of these set-ups are operated at atmospheric pressures (41) (35) (39) which makes them less suited for high pressures testing.

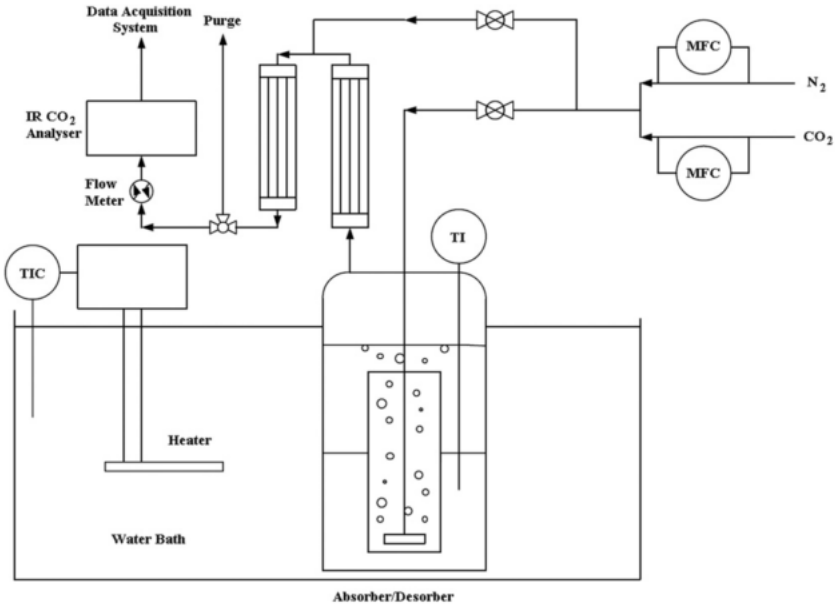

Figure 5 – Experimental set-up which allows for simultaneously determining the reaction kinetics and the CO2 loading (39)

To determine high pressure loading curves, an experiments set-up similar to the one shown in Figure 6 is used by various researchers. In this set-up, a unloaded solvent is loaded into the vessels. Next, the whole system is pressurized (using N_2 and CO_2) until the set pressure is reached. By rotating the vessels along its horizontal axis, mixing of the CO_2 and the solvent is achieved and the CO_2 is absorbed by the solvent. After a set time, the rotating is suspended and the liquid is removed for analysis. As the pressure and loading are known, this experiment can be used to determine the loading curve.

Even though accurate readings can be obtained while using this technique, a lot of time is required for the experiment as this is a batch process. Also adding additional CO_2 when the system is at equilibrium is not possible in the shown set-up.

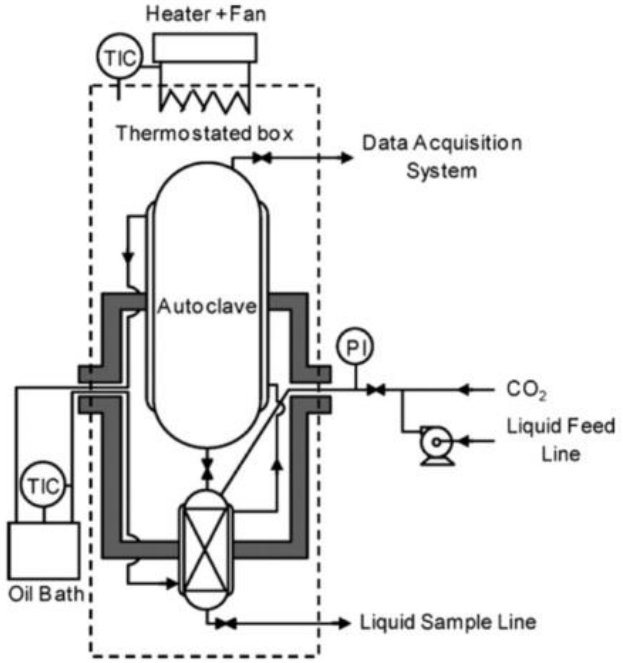

Figure 6 – High pressure CO2 loading set-up, used e.g. for determining CO2 loading curves (39)

The experiments described above all yield a solvent which has absorbed CO_2. However, the amount of CO_2 has to be determined as well in order to know the loading. The loading can be determined in a number of ways. The most straight forward is by using mass balances; a technique which is e.g. applied in Figure 5's set-up. Knowing the flow in and out of the reactor, the respective CO_2 concentrations and the amount of solvent are sufficient.

Conducting the experiments which have been described in Figure 5 and Figure 6 enables to determine the heat of absorption. By using the Clausius-Clapeyron (or Van 't Hoff) equation, the heat of absorption can be calculated when knowing the loading curves at various temperatures (48) (49).

However, this technique does not work when different loadings can exist within the same system, e.g. when two phases are present. One technique for such analysis has been proposed in 2008 by M. Hilliard (48) and is often revered to as the Total Inorganic Carbon analysis (TIC). This technique uses boiling phosphoric acid to strip the solvents and a gas analyser to measure the evolved CO_2; see also paragraph 3.4.2 for a more detailed description. This technique has since publication successfully been used in a number of research projects (16) (50) (51).

Another technique which has been used to determine the amount of CO_2 absorbed is FTIR. FTIR has been used for this purpose in relation with CCS (52) (53), but has also been used in many other fields for composition analysis of liquid and gaseous samples (54).

Furthermore, the temperatures at which the absorption is tested is very important for the maximal loading which can be achieved. Operation condition of most absorption columns are between 40 and 70 ^{0}C, while most strippers are operated between 100 and 140 ^{0}C (55). For that reason, many of lab experiments are conducted at these and intermediate temperatures to gather as much as possible data about e.g. amine degradation and loading at various temperatures (35) (39) (48) (56).

Finally, viscosity meters are used to determine the viscosity. No specific designs are given as viscosity meters – just like e.g. Karl Fischer titrations – can be found in most laboratories and come in various shapes and sizes. Some of the meters used are the Ubbelohde viscosity meters (used by Zhang et al. (28)) while Freeman et al. use cone and plate rheometers (50) to determine the density.

3 Methods & Materials

3.1 Narrowing down the scope and high pressure selection criteria

Based on the results of the reference experiment, the available apparatus and the results of the literature study, the scope of this thesis was narrowed down:

- Absorption kinetics will not be considered, as the available apparatus is not capable of determining these. Furthermore, this thesis is about increasing the general knowledge of high pressure phase splitting solvents; not about finding the optimal phase splitting blend. It is appreciated that such information about the reaction kinetics is very valuable when modelling this technique or designing a (pilot) plant. However, due to the nature of this thesis, time constrains and the lack of apparatus, these will not be experimentally determined. Instead, literature sources – when available – will be used for additional information.
- Degradation experiments will not be conducted, for the same reason why the kinetics experiments will not be conducted. Furthermore, a large amounts of data have been published about solvent degradation and – when required –will be used instead.
- The blend used will be a mixture of primary and tertiary amines, mixed with a physical solvent and water. During the reference experiment, a blend containing these chemicals has been used and proven to be successful. Since there is no information available to suggest otherwise, this composition will continued to be used.
- The viscosity will not be taken into account, as no suitable viscosity meter was available.

During the course of this thesis, one blend was selected to be tested at high pressures. The aim of this was to determine the effect of a high pressure on phase composition and loading. For this blend, the heat of absorption was also determined to enable a – preliminary – energetic analysis. Determining the heat for all phase splitting solvents would take a lot of time and would – without other high pressure data such as loading curves and phase compositions – have little additional value. Hence only the regeneration energy of the high pressure blend was determined.

The criteria to select one of the blends to be tested at higher pressures are largely given and explained in paragraph 2.3. As loading of the solvent is very important, this was one of the prime aspects when selecting a solvent to test at high pressures. The heat of absorption, reaction kinetics and amine degradation were also be considered, even though no experiments were conducted to experimentally determine these. Instead, literature sources were used for additional information to select between the blends which proved to split into two phases.

3.2 Amines and physical solvents used

As said, the mixtures used in the reference experiment was a mixture of a primary amine (AEP; 10 wt%[2]), a tertiary amine (MDEA; 15 wt%), a physical solvent (sulfolane; 50 wt%) and water (25 wt%). The chemicals presented in the tables below (Table 1 – 4) are based on scientific literature, design handbooks and in-house knowledge at TNO[3] and were used without any further purification.

Table 1 - Commonly used primary amines, based on scientific literature, design handbooks and in house knowledge

Primary amines			
Name	Acronym	CAS number	Reference
Monoethanolamine[4]	MEA	141-43-5	(13) (21)
Aminoethylpiperazine	AEP	140-31-8	(22)
2-amino-2-methyl-1-propanol	AMP	124-68-5	(28) (21)
Ethanediamine	EDA	107-15-3	(57)

[2] Unless indicated otherwise, mass percentages are used throughout this thesis.
[3] The lists of amines and physical solvents presented are non-exclusive, as there are other chemicals which can be used to obtain a phase change. However, the selected chemicals have been used extensively and hence (most) of their (CO_2 absorption) characteristics are known. Since the main objective of this thesis is to increase the knowledge about the observed phenomena instead of optimizing the solvent, only a limited number of solvents will be considered at this stage.
[4] The grade and supplier of the used chemicals and details about the equipment used during these experiments can be found in appendix A.

Table 2 - Commonly used secondary amines

Secondary amines			
Name	Acronym	CAS number	Reference
Piperazine	Pz	110-85-0	(21)
Diethanolamine	DEA	111-42-2	(13) (21)
Dipropylamine	DPA	142-84-7	(40)
N-methyl-1,3-diaminopropane	MAPA	6291-84-5	(27)
N-methylcyclohexylamine	MCA	100-60-7	(28)

Table 3 - Commonly used tertiary amines

Tertiary amines			
Name	Acronym	CAS number	Reference
Methyldiethanolamine	MDEA	105-59-9	(13) (21) (9)
Diethylethanolamine	DEEA	100-37-8	(27)
N,N-dimethylcyclohexylamine	DMCA	98-94-2	(28)
Aminoethylpiperazine[5]	AEP	140-31-8	(22)

Besides the amines, a number of physical solvent/processes have been identified which are currently used; see also Table 4:

Table 4 - Commonly used physical solvents

Physical solvents & processes			
Name	Active components (IUPAC and/or other common name)	Operating temperature	Reference
Sulfolane	2,3,4,5-tetrahydrothiophene-1,1-dioxide	n/a	(12) (13)
Selexol	A mixture of dimethyl ethers of polyethelyne glycol	Between 0 and 175 ^{0}C	(18) (9)
Purisol	N-methyl-2-Pyrrolidone	-15 ^{0}C	(18)
Sulfinol process	Diisopropanolamine with water and either sulfolane or MDEA	n/a	(9)
Hysweet process	Thiodiglycol (TDG) with either DEA or MDEA	n/a	(4)
Rectisol process	Liquid methanol	Max. -10 ^{0}C	(9)

For a number of reasons, a number of the described processes and solvents will not be used:

- *Rectisol*: the operating temperature of the Rectisol process are too low, as chemical absorption usually takes place at temperatures of about 40 ^{0}C (55). Combining these two concepts in a single column would technically be very difficult, therefore the Rectisol process will not be considered during this thesis.
- *Purisol*: This technique also requires operating at a temperature much lower that the temperature at which the chemical absorption takes place. Hence the Purisol process is not considered during this thesis.
- *Selexol*: Selexol is the trade name of a mixture of dimethyl ethers of polyethelyne glycol and is produced by several companies including the Coastal Chemical Company as Coastal AGR (18) and Union Carbide (58). Even though Selexol has several favourable characteristics (such as chemically stable and low vapour pressure (9), it has been patented by third parties. To prevent future difficulties, patented processes will initially not considered. The reason for this is that these might make future developments much more complicated. However, Selexol has some very favourable characteristics as a physical solvent, hence future developments might use Selexol as the physical solvent despite the current patents.
- *Sulfinol* process: the blend used in this process is very comparable with the blend used in the reference experiment. Since this blend will be extensively tested, it will not be considered separately.
- *Hysweet* process: given that process has been patented, it will not be used; for the same reasons that Selexol will not be considered. However, as TDG has not been patented as a physical solvent it will be tested as such.

[5] AEP has a primary and tertiary nitrogen atom. Hence it can be both a primary and tertiary amine, depending on e.g. how much time is given for absorption of the CO_2.

I.e., only sulfolane and TDG will initially be considered as physical solvents.

3.3 Experimental set-up description

During this research, a number of experimental set-ups have been used. In the next section, the operation procedures and calculations involved in each set-ups are described. After this section, all the experiments themselves are described and reference to this section will be made.

For both the low and high pressure experiments, a set-up was used which is different to the ones described in paragraph 2.4. This is mainly due to the need of conducting the screening experiments at elevated pressures. Also, the alternative designs allowed for a gradual pressure increase and hence easier determination of the loading curves when compared to the other designs.

3.3.1 Low pressure experiments

In order to rapidly screen the possible blends for phase changing properties, low pressure experiments were conducted. These experiments were conducted in a Mini AutoClave (MAC), which consist of 6 100 ml reactors with heating jackets and which were connected to a vacuum pump. A known amount of blend (ca. 50 ml.) was added to each of the reactors. The vacuum pump was used to remove as much of the ambient air as possible before heating and/or adding CO_2. This was done to achieve the highest CO_2 partial pressures. Also, vacuuming before heating the bled reduced the effects of evaporation of the blend as much as possible. Depending on the chosen reactor, a water or oil bath was used to keep the temperature constant at 40 ^{0}C while a magnetic stirrer was used to achieve proper stirring in the reactor. See Figure 7 for an schematic representation.

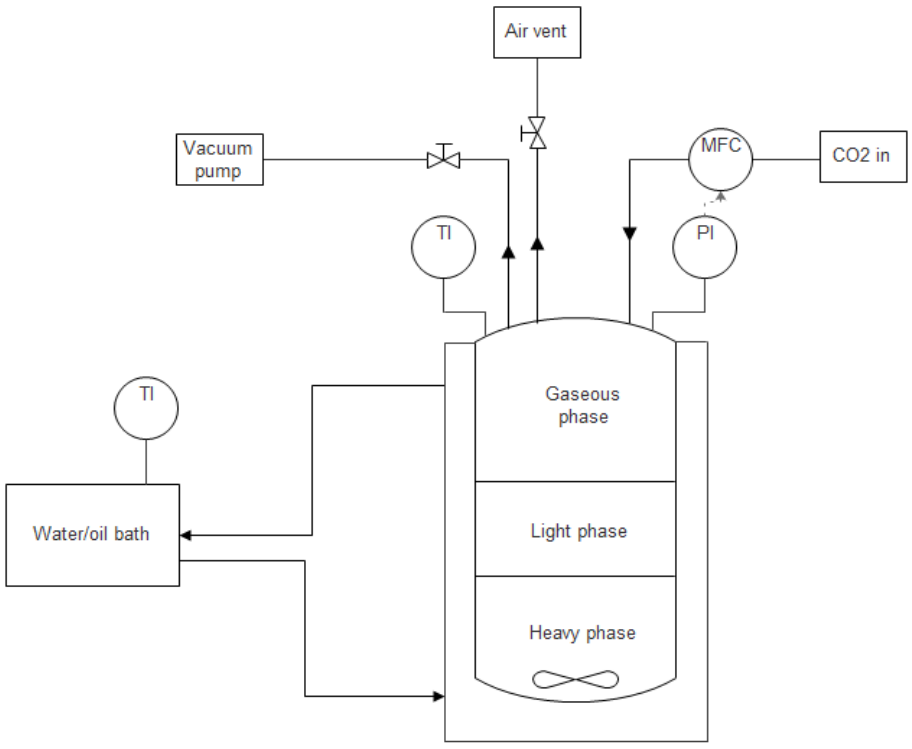

Figure 7 – Representation of one of the low pressure reactors which is part of the low pressure set-up ('MAC')

The experiment was started by injecting CO_2 (0,091 nL per step) into the headspace. This caused an initial pressure increase, after which is dropped due to absorption by the solvent. After some time, a stable pressure was reached; implying that no more CO_2 was absorbed; i.e. an equilibrium was reached. For these experiments, equilibrium was defined as less than 1 kPa fluctuations during a 10 minute period (TNO standard). Having reached equilibrium, a new pulse was injected, causing another pressure increase. This sequence was repeated until the pressure reached 550 kPa (TNO standard).

Once the pressure had exceeded 550 kPa, the experiment was ended. Having suspended the stirring and waited for 30 minutes, it was visually determined whether or not two phases were formed. Having established this, the MAC was depressurised since none of the follow-up experiments (loading, density) could be conducted in the MAC and/or while being pressurised. Having released the pressure, the reactors were emptied and cleaned. A separation funnel was used to separate the two phases for further analysis (Figure 8).

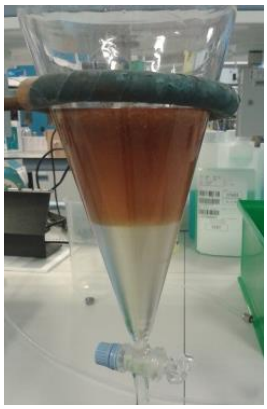

Figure 8 – Cone shaped separation funnel containing the loaded 2 phases solvent

3.3.2 High pressure experiments

To determine the performances at high pressure, a larger autoclave (VLE; Vapour-Liquid Equilibrium) was used. The VLE is essentially the same as the MAC since it consist out of a reactor which can be heated via an oil bath to a certain temperature, a (improved) stirrer is present and the reactor is connected to a vacuum pump to remove as much ambient air as possible before starting. See Figure 9 for a P&ID.

However, there are some essential differences between the two. The VLE contains 1) a larger volume (1000 ml, of which roughly 500 ml is the blend); 2) the CO_2 is injected directly in the liquid phase (instead of in the headspace, this allows for faster absorption); 3) a baffle is placed in the reactor (for improved mixing); 4) both a steel and glass reactor were used (the metal reactor was capable of withstanding pressures up to 60 bar; the glass reactor was used to closely monitor the absorption up to 5,5 bar) and 5) the VLE is equipped with more sensitive sensors.

As the design of the VLE is comparable with the MAC's, operating procedures are roughly the same. A vacuum pump was used to remove as much ambient air as possible before heating and/or CO_2 injection; the oil bath was used to keep the temperature constant; pulses of CO_2 were injected only if a stable pressure was reached (max. 10 kPa fluctuations in 10 minutes) and after reaching the maximum pressure (1.500 kPaA) the experiment was ended. The volume of the pulses varied due to differences in the settings between 0,036 and 1,47 nL per pulse. Even though this effected the time required to reach equilibrium, it is not believed that the position of the equilibrium itself was effected by this.

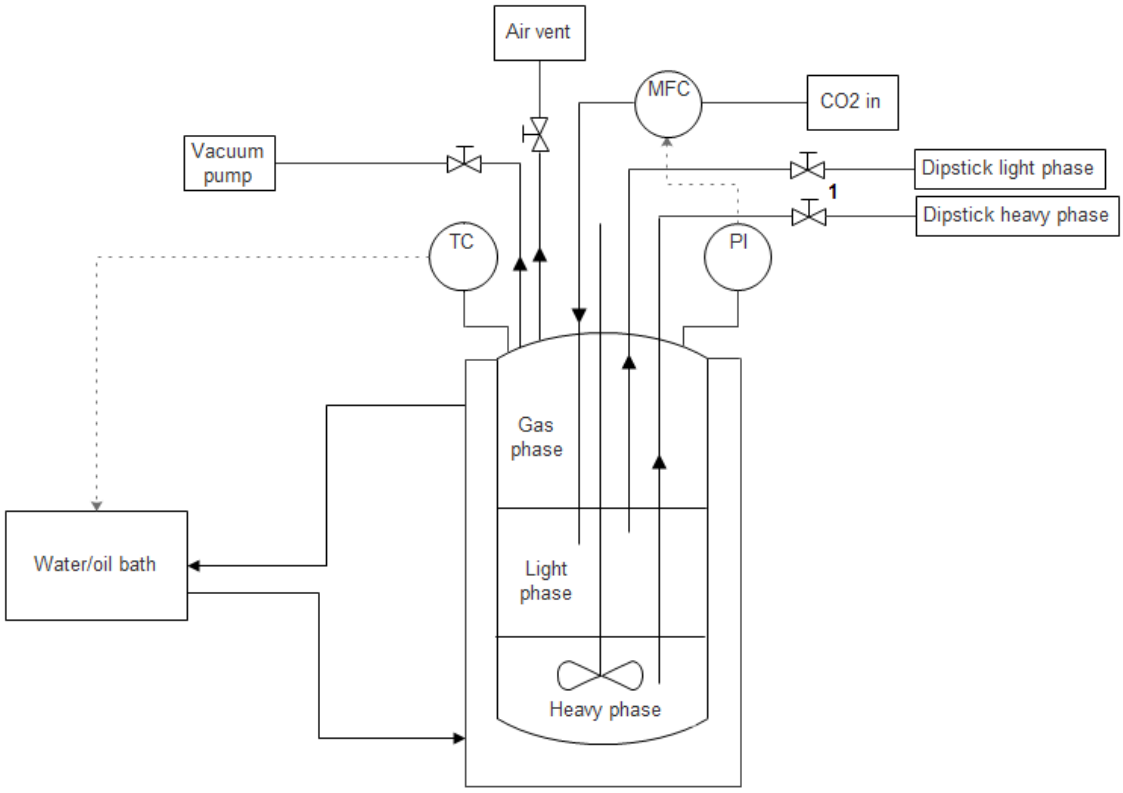

Figure 9 – High pressure experimental set-up ('VLE'). The dipsticks were used for sampling at high pressure but could also be removed when not being used.

Samples of each phase were taken in order to determine the composition of either phase. Samples were only taken when the system was at equilibrium; i.e. less than 10 mbar pressure changes in 10 minutes. To be able to take samples required that some small modifications had to be made. Two 'dipsticks' were designed, reaching from the seal to either the top of top phase or the bottom of the bottom phase via which pressurized samples of either phase were taken. See also Figure 9.

Having suspended stirring and having given the two phases enough time to settle, samples were taken by using these vacuumed sample tubes (see Figure 10). Swagelock piping was used to ensure a leak tight connection between the two was made. Next, valve one (see Figure 9) was opened. This was to ensure the connection between the sample tubes and dipsticks was airtight. Next, valve two (Figure 10) was opened to allow the samples into the sample tubes.

Figure 10 – Schematic representation of the used sample tubes

Removing about 4 ml of sample (i.e. the volume of the sample tubes) from the VLE caused the pressure to decreased and to stabilize at a new pressure. At this new stable pressure, valve three (Figure 10)a was slightly opened to ensure the whole tube was filled with liquid. Having confirmed this, all valves were closed and the test tube was removed. The other phase was sampled via the same procedure but by using the other dipstick; after which stirring continued and a new pulse of CO_2 was injected.

As said already, the sample tubes were vacuumed before taking samples. This was done to have the larger driving force between the reactor and the tubed; which should allow for faster sampling at especially low pressures. Furthermore, the sample tubes were used for density measurements. Having air left would spoil these measurements, as the density of air is roughly $1/1000^{th}$ of the density of the solvent. Hence, removing as much air as possible beforehand was considered to be necessary.

Due to the sampling, liquid was extracted from the reactor and – as a result – the pressure decreased. Even though relatively small sample volumes are involved (ca. 3 ml per sample), this change in volume was taken into account when calculating the loading.

3.4 Determining the CO_2 loading

As discussed, there are multiple methods which can be used to determine the loading. Now follows a description of the methods used.

3.4.1 Loading curves construction

As the number of pulses added and their volume are known, the amount of CO_2 added to the reactor was known. This enabled to calculate the loading of the blend, by using the ideal gas law and a mass balance:

$$CO2_{added} = \sum_{s=1}^{s} \Phi \cdot t = CO2_{absorbed} + CO2_{headspace}$$

Knowing the pressure and volume of the head space, the amount of gas in there was calculated by using the ideal gas law[6]:

$$CO2_{headspace} = \frac{P \cdot V_{headspace}}{RT}$$

The remainder of the CO_2 was absorbed by the blend; allowing the loading to be be calculated:

$$\text{loading} = \frac{CO2_{absorbed}}{V_{solvent}} \text{ or } \frac{CO2_{absorbed}}{n_{amines}}$$

With:

[6] The ideal gas law can be used to describe the relations between pressure, volume and temperature for perfect gasses. This formula works reasonably well for moderate temperatures and low pressures, as at high temperatures and pressures large deviations start to arise and alternative relations – such as the Van der Waals equation – has to be used. During this thesis, CO_2 is considered to be an ideal gas and – thus – the ideal gas law can be used.

S = number of steps added
Φ = volumetric flow rate (Ln s^{-1})
t = time of one pulse (s)
CO2 absorbed = CO_2 absorbed by the solvent (moles)
CO2 headspace = CO_2 in the headspace (moles)
P = CO_2 partial pressure in the headspace (Pa)
$V_{headspace}$ = headspace volume (L)
R = gas constant (8,314 J K^{-1} $mole^{-1}$)
T = temperature of the gaseous phase (K)
$V_{solvent}$ = volume of the solvent (L)
N_{amines} = moles of absorbing amines (mole)

Using these formulae, a CO_2 loading curve was constructed (see Graph 1). This shows the loading as a function of partial pressure; even though it is conventional to plot the partial pressure is on the Y-axis.

For all the high and low pressure experiments, the mass added to the reactors and the liquid density were determined. Hence, differences in the amount of blend added (and based on this: differences in loading) were accounted for. Furthermore, a pressure of ca. 10 kPa A was reached when removing the air from the VLE and MAC via the vacuum pump. By recording this pressure, this was also accounted for when calculating the CO_2 partial pressure.

Note that the total loading of the solvent was presented as moles of CO_2 absorbed per litre of blend. This is contrary to what is conventional; i.e. mole CO_2 per mole amine. However, since as a mixture of physical and chemical solvent were used, it was not considered to be representative to allocate all the absorbed CO_2 to the amines. Hence, the loading is presented in terms of moles of CO_2 absorbed per litre of blend. If necessary, literature figures will be presented in this unit as well, to accommodate easy comparison.

Graph 1 - CO2 loading curve, which is based on the pressure in the reactor and the amount of blend added

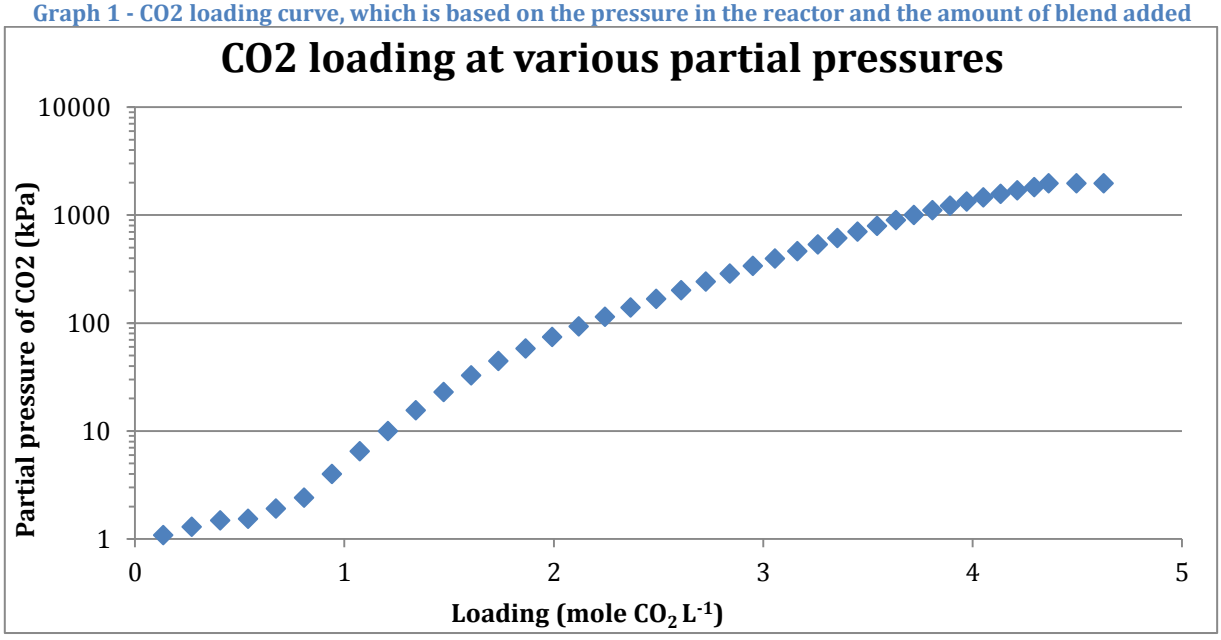

3.4.2 Boiling phosphoric acid

By using data from the MAC and VLE, the amount of CO_2 absorbed by the blend as a whole is calculated. However, this provides little information about the loading of each phase. Instead, this was determined by using boiling phosphoric acid. A known volume of loaded solvent was added into a flask containing boiling phosphoric acid. As a result, both physically and chemically absorbed CO_2 were stripped from the solvent. A flow of pure nitrogen was used to dilute the gas and to connect the flask to a gas analyser. Depending on the total amount of sample available, the flow of nitrogen could be varied to test samples of various sizes. See also Figure 11 for a flow diagram of the experimental set-up.

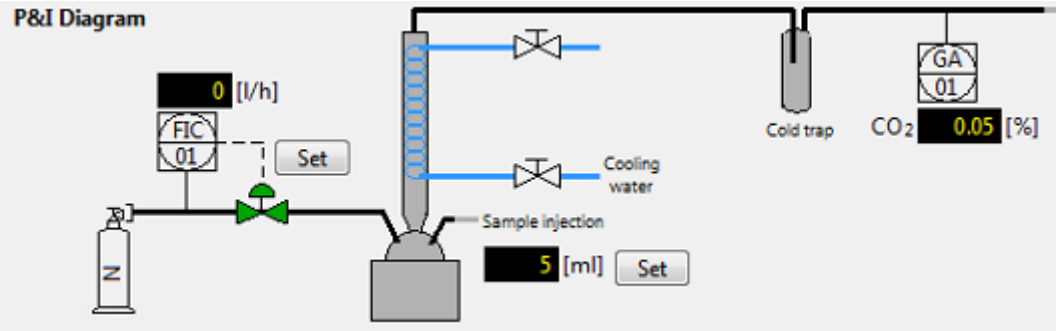

Figure 11 – Phosphoric acid experimental set-up

Since chemically absorbed CO_2 forms carbamates with the amines, depressurizing is believed to have only a limited effect on the loading of the chemical phase; even though some physical absorbed CO_2 could also be present. For that reason it was assumed that the loading of the chemical phase could accurately be determined.

However, this cannot be said from the physical phase. Reducing the pressure is how the solvent is regenerated; essentially what happened when the blend was removed from the MAC/VLE. Hence, most of the absorbed CO_2 flashed off while removing the blend from the reactors. As a result, the loading of the physical phase could not accurately be determined.

3.4.3 ATR-FTIR analysis

An alternative method to determine the loading is by using Attenuated Total Reflection Fourier Transform InfraRed analysis (FTIR for short). As each molecule has a unique chemical structure, the IR absorption spectrum of each structure is also unique. Hence, this method can – after calibration – be used to identify components (such as amines and CO_2) and their concentration within a mixture.

For the calibration, ca. 500 ml of the light phase was made (the composition was based on the GC analysis), which was split into two equal parts. One part was left during the weekend to be fully loaded (at atmospheric pressure) while the other part remained unloaded. The phosphoric acid experiment was used to determine the loading (3,45 mole L^{-1}); while the absorption spectrum of the loaded phase was also analysed. By diluting the loaded phase with the unloaded phase, various loadings were achieved while the concentration of all the other components was kept constant. After each dilution step, the absorption spectrum was analysed as part of the calibration. For the calibration, the wavenumbers (i.e. cm^{-1}) between 800 and 2.500 were considered.

3.5 Phase composition analysis

In order to determine the composition of the two phases, a gas chromatograph and Karl Fischer titrations were used. Analysis of either phase was conducted as the composition of the phases is important for CO_2 stripping. A high amine concentration in the physical phase will significantly reduce the advantage of pressure swing absorption and thus the possible gains in e.g. energy efficiency[7].

3.5.1 Gas chromatograph analysis

A Gas Chromatograph equipped with an flame ionizing detector (FID) was used for the qualitatively and quantitative analysis of each phase. The first step in this process was to determine whether or not the GC was capable of detecting the various components within the samples. This was done by analysing the pure components which were diluted with ethanol.

Ethanol was chosen as dilutant as ethanol doesn't interfere with the sample, has different retention time than the analysed components and is readily available. Furthermore, by diluting the sample less sample had to be injected which ought to reduce the pollution of the column. Finally, dilution of the samples ensured the concentrations being within the working limits of the GC.

[7] A high physical solvent concentration in the chemical phase is not considered to be as troublesome. First off all, the stripper is operated at a lower pressure – compared to the absorber – hence flashing most physically absorbed CO_2.

By using samples with various concentrations (ranging from 1 % up to 100 %) the GC was calibrated for the quantitative analysis. The area under the curve for each component was directly proportional to the concentration in the liquid (see also Appendix B – gas chromatograph). This linear relation between extinction and concentration enabled easy concentration calculations of either phase.

Each sample was accurately diluted roughly 60 times using an analytical balance and high grade ethanol. Before injecting 1,0 µL of the diluted sample into the GC, the syringe was rinsed 4 times to remove any old samples which might still be present. The same syringe was used throughout the project, as different syringes might lead to differences in the amount of volume injected.

Furthermore, the blend itself was analysed[8] to make sure no overlap existed between the various components and to validate the calibration lines which had been constructed. The results of this validation can be seen in appendix C.

3.5.2 Water content

As the GC was equipped with an FID, water could not be detected or measured. Instead, a coulometric Karl Fischer titration was used to do so. By measuring the electric current which is required to sustain the reaction in which water reacts, the amount of water is determined (59).

Based on the water content of the original blend it was anticipated that the water content of either phase was relatively large (> 5%). Hence, the diluted samples which were used for the GC were also used to determine the water content. This should give more accurate results, as the set-up is most accurate between concentrations of 1 and 10.000 ppm (59). Furthermore, a lower concentration should recue the time required for the analysis as less water has to react. Using diluted samples should not have any effect on the quality of the results as high grade ethanol[9] was used containing very little water or other components.

For the Karl Fischer experiments, there should be little difference whether methanol or ethanol is used as solvent (59). Furthermore, current developments are that ethanol is used to replace methanol in the Hydranal® reagent line (60) as ethanol is less toxic. This implies that there is little difference between using either, which is something which will be tested as well.

3.6 Density measurements

Many liquid-liquid separators use a difference in density as the driving force to separate between the two phases. The larger the difference in density is, the faster, easier and better separation will be (61) (62); especially when the two phases have been thoroughly mixed in e.g. an absorption column.

Hence, the density of both phases was measured. The density of the pressurized chemical phase was believed to be same as the density at atmospheric pressure. However, the density of the physical phase at atmospheric pressure was not considered to be reliable. Decreasing the pressure caused the physical phase to flash while the changes in mass and volume could not be measured. As a result, the density of the physical phase at atmospheric pressure varies from the density when pressurised. However, these can be used to compare the various physical phases with one another.

The samples obtained during the screening experiments were sufficiently large that a standard density meter could be used to determine the density. The density was measured at 40 ^{0}C , since this was the operational temperature of the MAC. Before using the density meter, a sample of demi water was analysed to make sure that the meter was clean and still working properly.

The density at high pressures initially measured using the same sample tubes (essentially small pieces of metal tubing with valves on either side) which were used to obtain the samples for phase composition analysis. As their volume was known, knowing the increase in mass was sufficient to

[8] Since the blend consists of the same components as the samples of the two phases, it is not considered to be a problem that the blend was used in this stage instead of actual samples.
[9] See appendix A for the grade of each of the components used.

determine the density. Key in this method is being certain that the sample tubes are completely filled when recording the mass increase; in paragraph **Fout! Verwijzingsbron niet gevonden.** more information about this can be found.

An alternative method to determine the density was based on using pipettes. Pipettes were used to take a known volume of the pure samples and determine the change in mass. Based on these measurements, the density was determined. For each sample, two measurements were conducted: the first was based on removing a known volume while the second was based on pipetting the known volume back. By averaging the results, the density was also determined.

3.7 Low pressure screening experiments

A total of 72 possible blends (9 primary amines, 4 tertiary amines and 2 physical solvents) were identified to be tested. In order quickly determine which blends do and don't cause a phase split, low pressure screening experiments were conducted in the MAC. These experiments were conducted at 40 ^{0}C, since this is the temperature at which many columns are operated.

The composition of reference experiment was taken as the starting point, since this blend has proven to split into two phases. The physical solvents was the first variable to be tested, before varying the tertiary amines and – ultimately – the primary amines. This sequence was chosen as this enables for rapid selection and cancelation of blends if no two phases – or not the desired phases – are formed.

Furthermore, the concentrations of the physical solvent and tertiary amine were changed to see the effect this might have as a large volume of physical solvent were required by the reference experiment; see also Table 5. The amount of physical solvent was reduced while the increasing the tertiary amine concentration to determine the effect of this.

Table 5 - Composition of the blends tested during the MAC experiments

Compound	Reference experiment	Alternative composition
Primary amine	10 %	10 %
Tertiary amine	15 %	30 %
Physical solvent	50 %	35 %
Water	25 %	25 %

3.8 High pressure experiments

Since the VLE consist of a larger volume, more accurate sensors, dipsticks and can handle a higher pressure, a number of additional characteristics have been determined. These include the identification of the tipping point and the composition of each phase at various CO_2 pressures which have – besides the loading curves – been identified.

3.8.1 Tipping point

The tipping point was defined as the CO_2 partial pressure at which the single phase system turned into a biphasic system. By using the glass vessel and by injecting small pules of CO_2 and wait for equilibrium to arise, this point was identified.

After reaching a stable pressure, stirring was suspended in order for the phases – which were assumed to exist –to settle. Having waited for 30 minutes without the two phases being formed, a new pulse was injected and the stirring continued. This sequence was repeated until two phases were formed, hence determining between which partial pressures (and thus loadings) the tipping point lies.

3.8.2 Loading curves of the light and heavy phase

During the high pressure experiments, various compositions have been tested. Initially, the composition of the low pressure experiments was used for the high pressure experiments. However, the VLE was also used to determine the loading curves of the light and heavy phase. The blends which were tested during these loading curve experiments were based on the results of the GC analysis of the samples.

3.9 High temperature experiments

Using the results of the GC analysis, a copy of the light phase was made which was used to determine the loading at high temperatures. These experiments were conducted in the MAC (see paragraph 3.3), in order to construct the CO_2 loading curve of the light phase at various temperatures. The experiments were conducted at three temperatures: 40 ^{0}C, 120 ^{0}C and 80 ^{0}C (intermediate between the high and low temperature), with a maximum pressure of 550 kPa A.

Since only the chemical phase will the thermally stripped, this is the only phase which was tested at elevated temperatures. As stated before already, regeneration of the physical phase is achieved by removal of the pressure. Hence, the loading of the lean solvent have already been determined using the FTIR and phosphoric acid experiments.

3.10 Heat of absorption

Using a modified version of the Van 't Hoff equation, the heat of absorption can be estimated. Using the expression as derived by Kim et al. (49) and Atkins et al. (63), the heat of absorption can be determined using the equation

$$\ln\left(\frac{P_2}{P_1}\right) = \frac{\Delta H}{R}\left(\frac{1}{T_2} - \frac{1}{T_1}\right)$$

With
P_1 & P_2: CO_2 partial pressures at equal loading (kPa A)
ΔH: heat of absorption (J mole CO_2^{-1})
R: gas constant (8,314 J K^{-1} $mole^{-1}$)
T_1 & T_2: temperature (K)

To use this equation, it is necessary to use the partial pressures at the equal loading to determine the effect of various temperatures. The loading curves were used in order to estimate the pressure at various loadings; linear interpolation was used to estimate the pressure at intermediate loadings.

This equation assumes the heat of absorption being independent of the temperature. However, this is not the case and thus inaccuracies are introduced. By using the average heat of absorption this was accounted for.

3.11 Regeneration energy

Knowing the regeneration energy enables to determine the amount of heat required to capture one mole of CO_2. This involves analysing the most energy consuming stages of the capture and stripping process. For most capture processes, there are three energy consuming stages which add up to approximates the energy consumption during capture (46):

- Raising the light phase's temperature from 40 to 120 ^{0}C;
- Endothermic reaction to strip the CO_2 is from the solvent;
- Evaporation of water in the stripper.

In order to estimate these three terms, additional information about the described process was required:

- The cyclic loading of the solvents
- Specific heat capacity (CP value) of the light phase
- Heat exchanger efficiency

The cyclic loading is defined as the difference between the lean and rich loading; i.e.

$$cyclic\ loading = loading_{rich} - loading_{lean}$$

Given that the chemical phase is a mixture of multiple components, the of the Cp was estimated via using the Cp value of the phase's constituents and their mass fraction:

$$CP_{light\ phase} = \sum_{s=1}^{s} x \cdot Cp$$

With:
s: each of the blend's components
x: mass fraction (%)
Cp: specific heat (kJ gr^{-1} K^{-1})

Due to the high stripper temperature, water will start to boil and evaporate. Using the heat of evaporation, the amount of required energy for this process was calculated as well.

For simplicity reasons, certain assumption were made to rapidly estimate the energy consumption of the plant and to compare the results to an aMDEA simulation (64). These assumptions are:

- All the energy is consumed during the three thermal processes; additional energy requirements (e.g. pumps, fans, etc.) were ignored;
- The absorber is operated at 7.000 kPa with a CO_2 partial pressure of 700 kPa A
- Both the chemical and physical phase were fed at the top of the absorber and tapped off at the bottom (see Figure 12 for a schematic process design);
- The lean chemical phase entering the top of the absorber column is at equilibrium with the CO_2 partial pressure;
- How much is absorbed by each phase is equal to the volume ratios of the two phases;
- Phase separation is instantaneous and perfect;
- There is no energy required to regenerate the physical phase;
- CP values are independent on temperature;
- The minimal temperature difference between the rich and lean flow flowing through the heat exchanger is 5 ^{0}C;
- Per mole of CO_2 one mole of water evaporates;
- The stripper is operated at 120 ^{0}C and a pressure of 180 kPa while the top of the stripper has a temperature of 105 ^{0}C due to reinjection of condensed water;

The result of these estimates was that a lot accuracy was sacrificed. As a result, the number obtained should not be used as a fixed number but rather as an estimate of the order of magnitude.

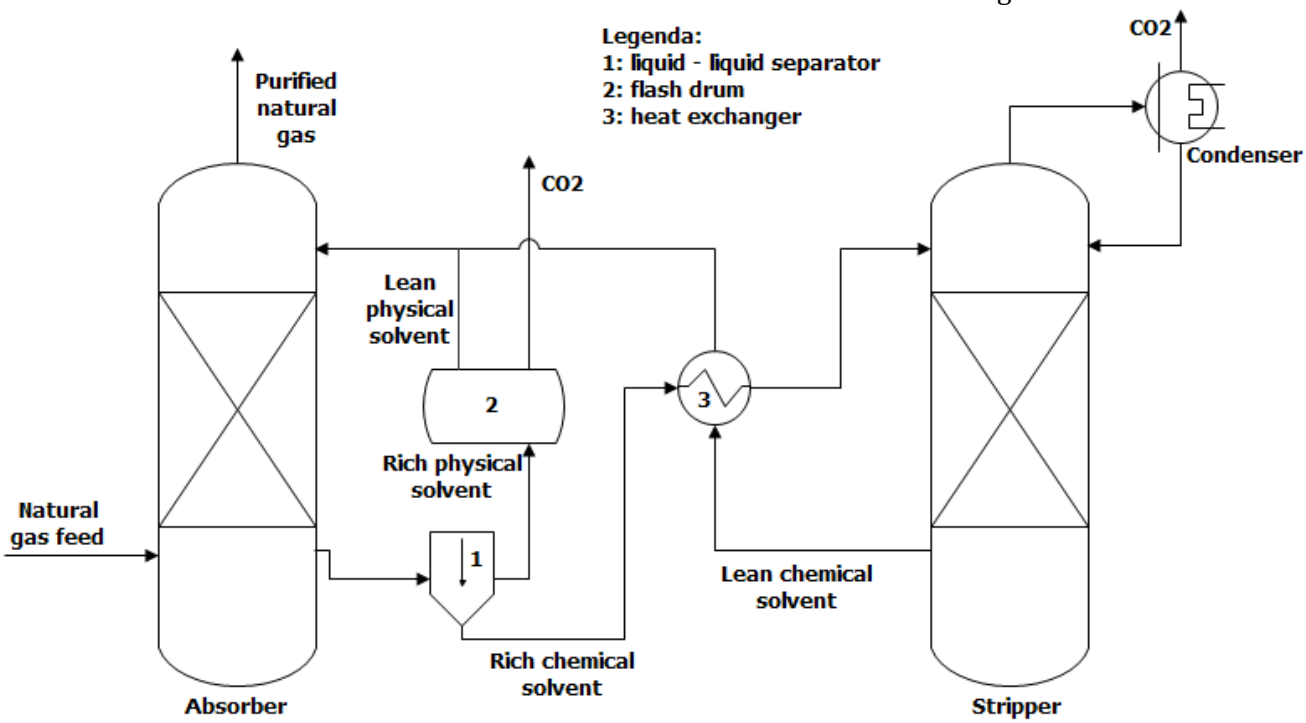

Figure 12 – Schematic process design of a two phase carbon capture plant. The major differences with a conventional capture plant are the phase separator (1) and flash drum (2).

4 Results & discussion

4.1 Low pressure experiments

Using the MAC, the first experiments were to determine whether or not a phase split occurs; i.e. the screening experiments. These experiments were conducted in twofold for increased accuracy. Of those blends which formed two phases, the loading and density of every phase were determined.

4.1.1 Phase split yes or no

The first experiment involved varying the physical solvents, to determine its effect on two phases being formed. Furthermore, the concentration of the amines and physical solvents were varied, in order to determine whether or not this had any effect on the phase split or loading. See Table 6 for the summary of the composition and results; photographs of experiments 1 – 6 can be found in appendix D; see appendix E for the experiments 7 – 13.

Table 6 - Screening experiment to determine the influence of composition and physical solvents

	Primary/secondary amines		Tertiary amine		Physical solvent		Water	
Sample number		Concentration (%)		Concentration (%)		Concentration (%)	Concentration (%)	Phase split?
Ref. exp.	*AEP*	*10,0*	*MDEA*	*15,0*	*Sulfolane*	*50,0*	*25,0*	*Yes*
1	AEP	9,6	MDEA	14,6	TDG	50,7	25,1	No
2	AEP	10,0	MDEA	28,3	Sulfolane	33,1	28,7	Yes
3	AEP	10,0	MDEA	31,2	TDG	34,0	24,8	No
4	AEP	10,1	AMP	15,9	TDG	49,2	24,8	No
5	AEP	10,1	AMP	30,2	Sulfolane	34,6	25,1	Yes
6	AEP	10,7	AMP	29,9	TDG	34,5	24,9	Yes

As can be seen from the table, there were three experiments which showed a phase split. However:

- Experiment 5: During the original experiments and the duplo, solids were formed at the liquid-gaseous boundary. Even though a two phases are formed, this isn't the desired result as two liquid phases are desired. For that reason, this mixture will not be taken into consideration[10].
- Experiment 6: As with experiment 5, two phases were formed. However, the result was an gel like substance instead of the anticipated liquid. Even though the solvent separate into two phases, this was not the separation as was desired and thus this blend will not be considered.

Given the results of these experiments, only sulfolane has been considered as the physical solvent. The next step was 1) to vary the tertiary amines and 2) vary the primary/secondary amine to see if this had any effect. See also Table 7 .

Table 7 - Screening experiment to determine the influence of primary, secondary and tertiary amines

	Primary/secondary amines		Tertiary amine		Physical solvent		Water	
Sample number		Concentration (%)		Concentration (%)		Concentration (%)	Concentration (%)	Phase split?
7	AEP	10	DEEA	15	Sulfolane	50	25	N/A[11]
8	AEP	12,0	DMCA	14,9	Sulfolane	48,4	25,6	No
9	MEA	11,0	AMP	14,7	Sulfolane	51,5	23,8	Yes
10	MEA	11,3	MDEA	15,4	Sulfolane	48,6	26,0	Yes
11	DEA	11,4	AMP	15,4	Sulfolane	48,9	25,3	No
12	DEA	10,8	MDEA	14,9	Sulfolane	49,6	25,8	Yes
13	Pz	9,2	MDEA	14,2	Sulfolane	46,3	31,3[12]	Yes

[10] Blends containing AMP have been reported to form precipitates when absorbing CO2, which might be what has happened in this experiment. See for example the paper by Svensson et al. (76)

[11] When starting the MAC experiments – no DEEA was available. Thus it was decided to postpone this experiment to a later stage. However, before the experiment could be conducted the MAC experiments were finished. Hence, no result for this experiment was obtained

[12] Since piperazine was difficult to dissolve, additional water was added. The blend which was used contained 31,3 % water, compared to ca. 25 % of the other blends.

Based on experiments 1 – 13, it was concluded that the composition is important for the phase split to occur. There are indications that a tertiary amine (possibly MDEA) has to be in the presence of sulfolane and a primary amine in order to obtain the split. However, more experiments are required for a more definitive answer. Based on the results in tables Table 7 and Table 8, no further screening experiments were conducted as these give an indication of the blend requirements.

4.1.2 Density & CO_2 loading

Of all the blends tested during the screening experiments, those who formed two phases were analysed further. Using the phosphoric acid setup and density meter, the CO_2 loading and density of each phase were determined.

Table 8 - Density of the unloaded solvent, the combined loading of the chemical and physical phase and loading and density of both phases.

			Chemical phase		Physical phase	
Sample number	Density unloaded blend (g ml^{-1})	Combined loading of the two phases (mole L^{-1})	Density (g ml^{-1})	Loading (mole L^{-1})	Density (g ml^{-1})	Loading (mole L^{-1})
2	1,097	2,668	1,200	3,23	1,251	0,01
9	1,111	2,377	1,191	2,86	1,250	0,05
10	1,123	3,270	1,191	2,84	1,246	0,08
12	1,134	1,675	1,186	1,80	1,244	0,10
13	1,119	2,127	1,186	2,86	1,239	0,06

The table shows that – on average – the density of the heavy phase is at ambient conditions ca. 5% larger than the density of the chemical phase. It is expected that the density difference for the pressurised phases is larger due to the physical absorbed CO_2. Estimating the physical phase's loading involved estimating the volume ratios of the two phases. As these could not be accurately estimated, these numbers have been left out.

It is interesting to notice that the two phases continue to coexist after the pressure is removed. This shows that after the two phases have been formed, no minimum partial pressure is required to sustain the phase split. This might partly be due to the chemically absorbed CO_2, which remains bound to the amines even though the pressure was released. However, the exact cause of this lies beyond the scope of this research and will therefore not be addressed, even though this can be valuable information when further developing this technique.

4.2 Solvent selection

As indicated in the previous paragraph, there are a number of blends which split into two. Based on the loading of each blend, blend 10 (10% MEA, 30% MDEA, 35% sulfolane, 25% water) would be the most favourable to test at high pressure since it has the highest loading (3,27 mole CO_2 L^{-1}).

However, MEA is sensitive to (thermal) degradation (65) during normal operations, like most of the tested chemicals. Compared to MEA, blend 2 (AEP, MDEA, sulfolane and water) is a blend which is less subject to thermal degradation. According to various sources, AEP is – just as MDEA – (66) is relatively inert in terms of thermal degradation (67).

Based on this, the reference mixture and blend 2 are the preferred blends for high pressure testing. As blend 2 has a higher loading than the reference mixture (previous experiments have shown determined the loading of the reference experiment to be 2,10 mole L^{-1};), blend 2 was used during the high pressure experiments.

4.3 High pressure experiments

Using the VLE, the MDEA/AEP/sulfolane blend (blend 2) has been tested. Two complete runs (an original and duplo) were conducted for increased accuracy; the low pressure runs in a glass vessel and high pressure runs a metal vessel.

Initially, the glass vessel was used since this enables for better observations, e.g. whether the dipsticks had been designed correctly and identification of the tipping point (see also Figure 13). Based on the

MAC results, it was known that the tipping point is less than 550 kPa. By adding small amounts of CO_2 at a time, the tipping point was observed to lie between 107,8 and 109,3 kPa partial CO_2 pressure. The duplo experiment confirmed this by indicating that the tipping points lies just below a partial pressure of 109,9 kPa. These partial pressures corresponds to a loading of approximately 2,15 mole CO_2 L^{-1}. This is less than the maximum theoretical amine loading of 2,90 mole[13] CO_2 L^{-1}, which indicates that AEP and MDEA are not yet saturated when forming two phases.

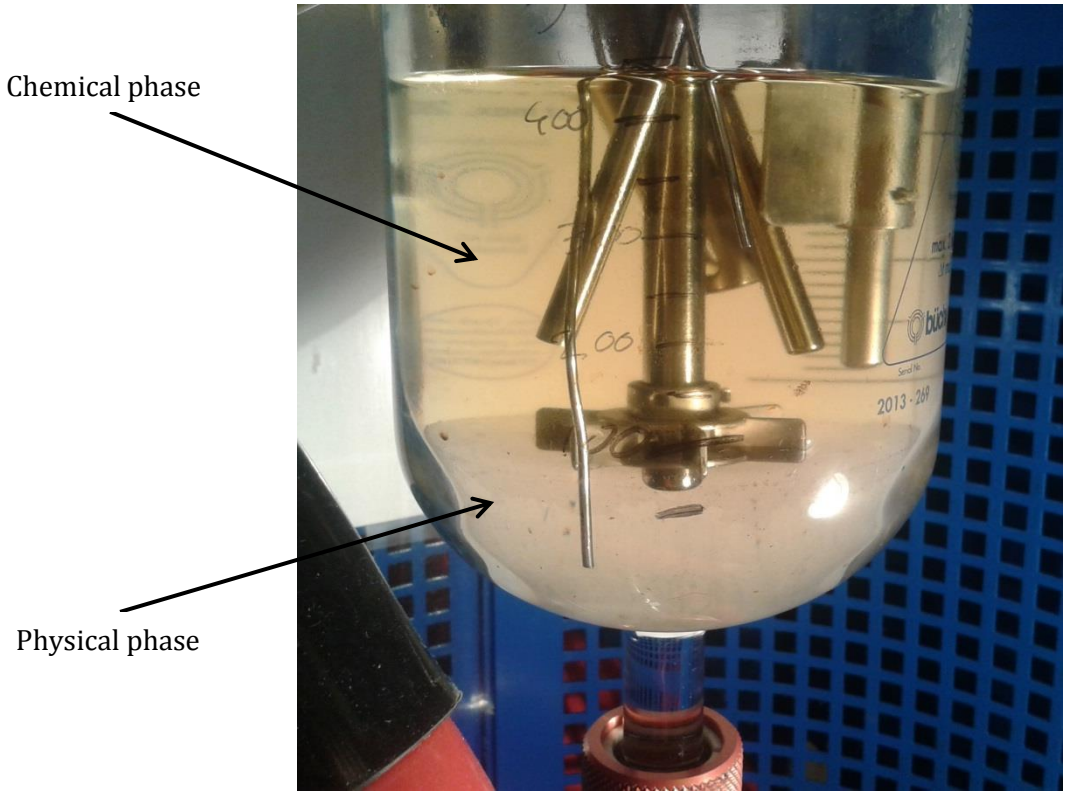

Figure 13 – Two phase system at CO_2 pressures just above the tipping point

Graph 2 shows the CO_2 loading curve of the blend, in which the results of the high and low pressure testing are combined. The linearity at high partial pressures can be explained with the physical solvent absorbing the CO_2. Furthermore, the original and duplo experiment are very close to one another, which gives confidence in the conducted experiments. During the VLE experiments there has been a 'original' and 'duplo' run; both starting at a vacuum and increasing the pressure to ca. 1.500 kPa. The duplo run revers to the second run during which samples were taken; it does not refer samples of the orginal run being analysed again. All the data obtained during these experiments can be found in appendix G.

In order to safe time, the low pressures runs have been conducted before changing to the metal reactor. By doing the experiments in this order, changing from the glass vessel to the metal vessel was only once conducted. Therefore there were less changes of leakage within the system.

The points in Graph 2 indicate the pressures at which samples were taken from the vessel. There pressures correspond to pressures at which the composition of the phases was determined.

[13] assuming a MDEA loading of 1 mole/mole and AEP loading of 0,5 mole/mole

Graph 2 – Loading curve of the AEP/MDEA/sulfolane/water blend. The graph shows the results of both the low and high pressure experiments, besides showing the general trends and the quality of the duplo.

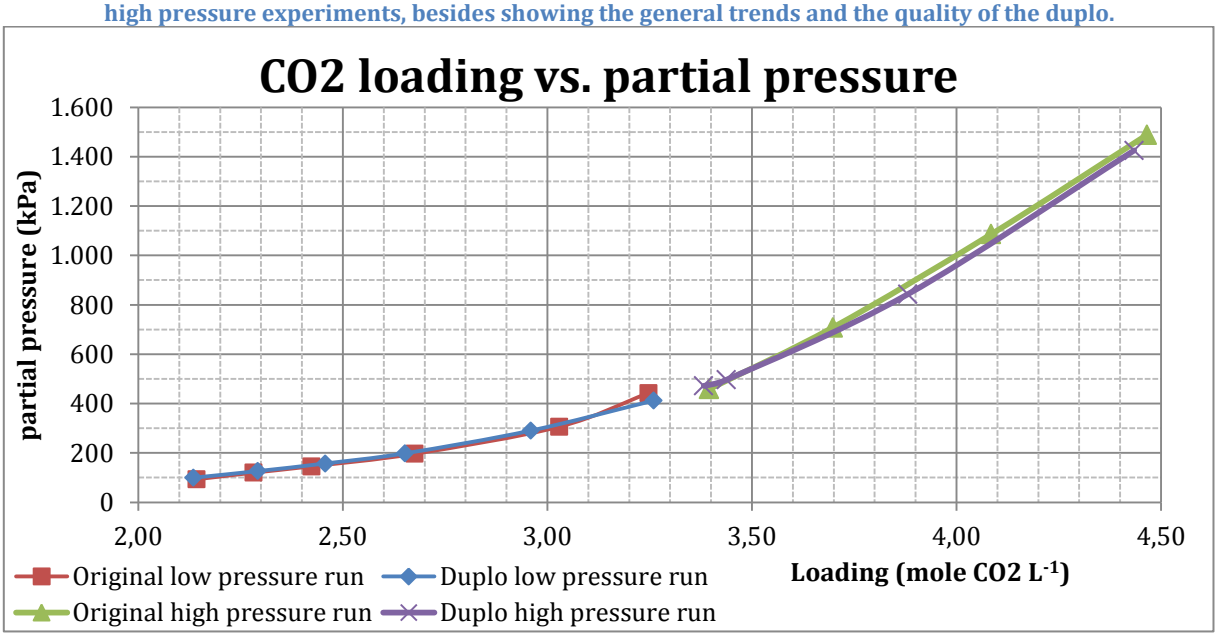

4.3.1 Phase composition

Using the GC and the Karl Fischer titrations, the composition of both the chemical and physical phase were determined. Figure 14 shows the identification of amines and physical solvents which were used. It can be clearly seen that the peaks of the components do not overlap. How the composition differs at various pressures can be seen on pages 30 to 35. The calibration curves which were used to determine the concentration in the samples can be found in appendix B while appendix C shows validation measurements of the blend to determine the offset between the two.

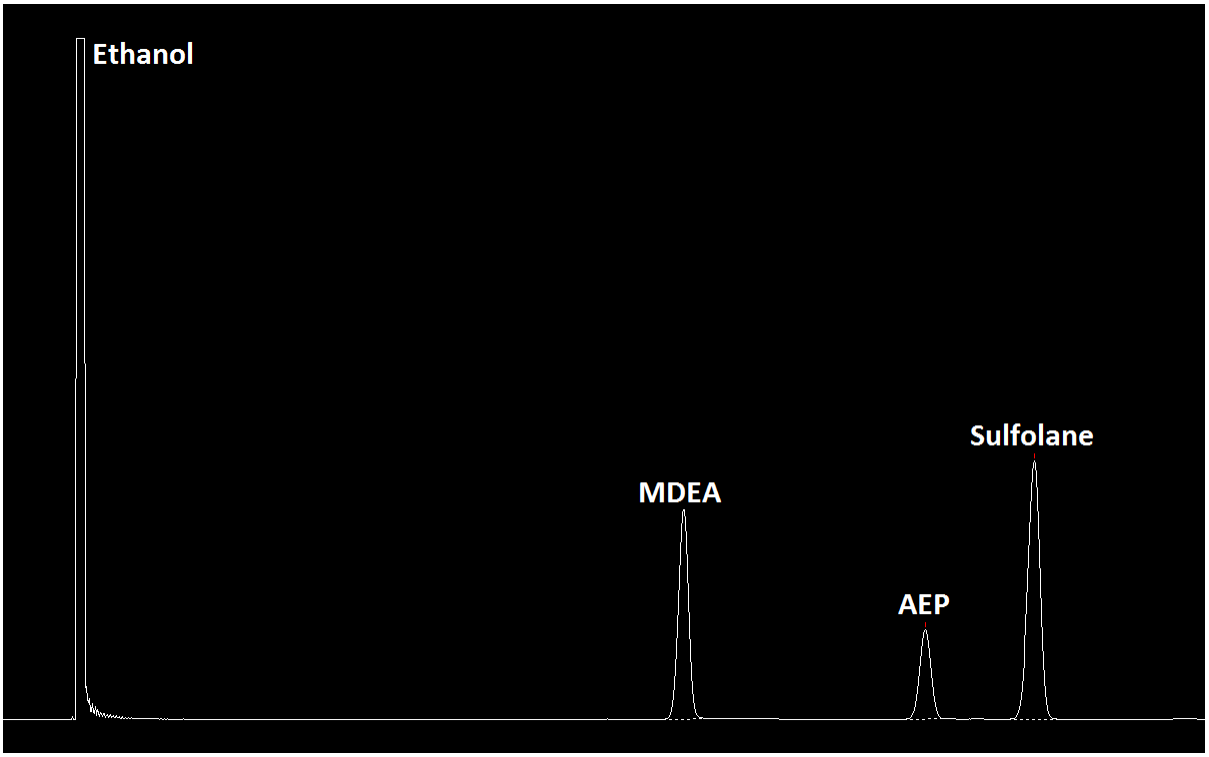

Figure 14 - Chromatogram of a sample containing MDEA, AEP and sulfolane with ethanol as solvent

4.3.1.1 Aminoethylpiperazine (AEP)

Graph 3 – AEP concentration in the light (chemical) phase at various CO_2 pressures

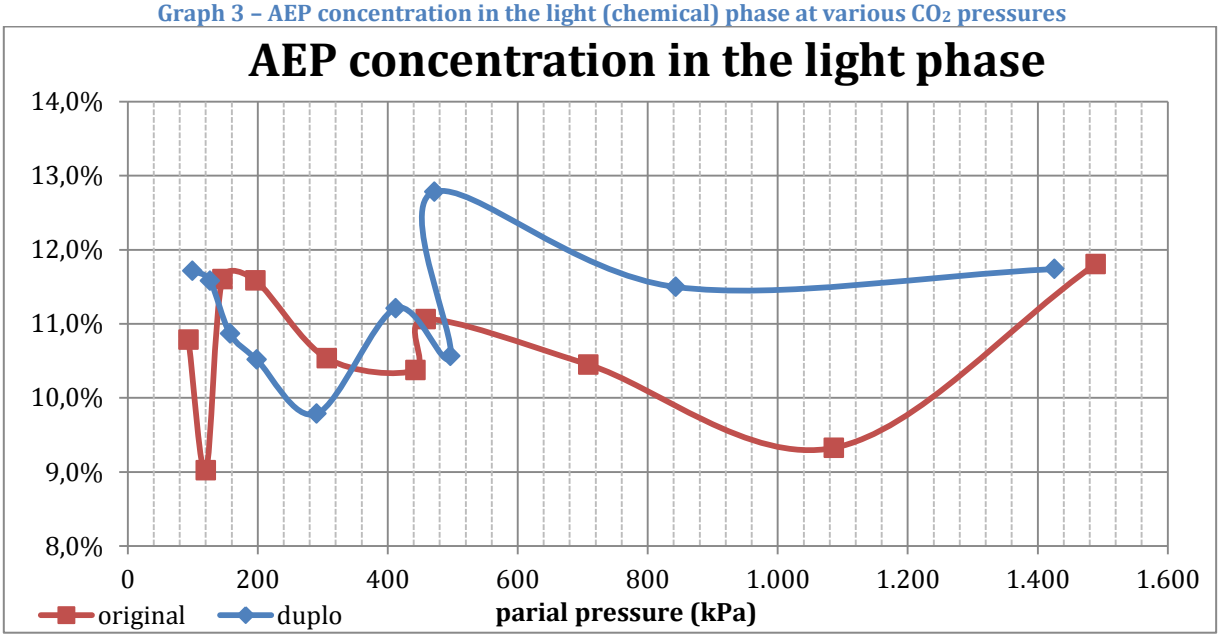

Graph 4– AEP concentration in the heavy (physical) phase at various CO_2 pressures

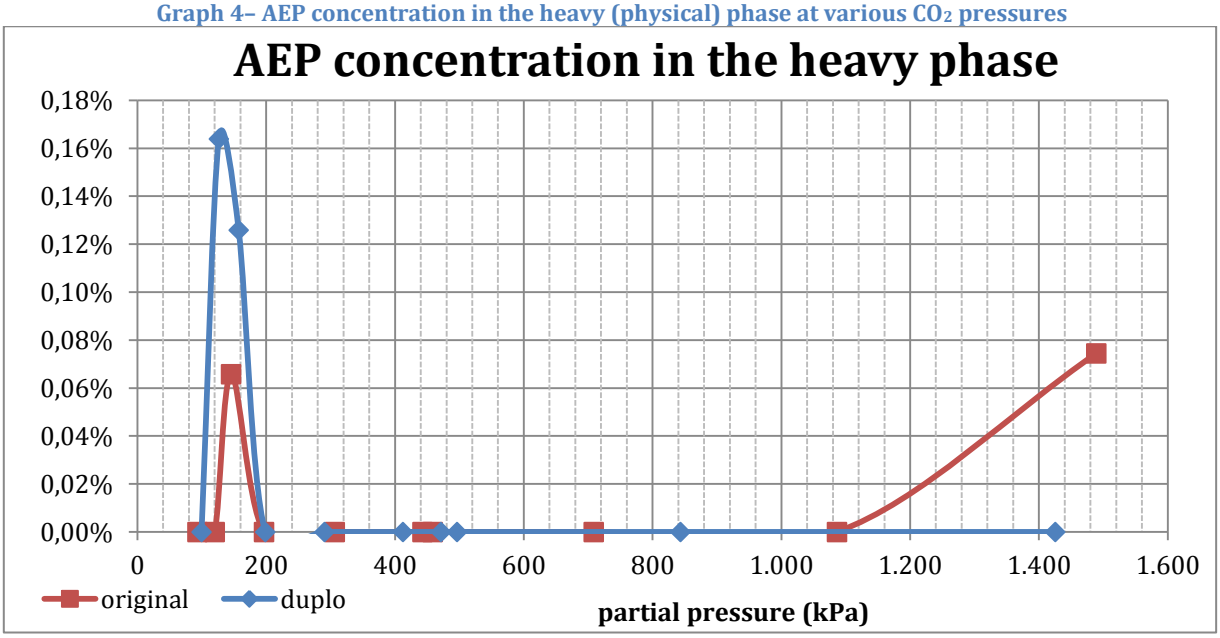

Graphs Graph 3 and Graph 4 show the AEP concentration at different partial pressures. From these graphs it becomes apparent that almost all the AEP can be found in the chemical phase while in the physical phase almost no AEP is present. The concentration in either phase appears to be independent of the pressure.

For the light phase the AEP concentration appears to be independent of the pressure; based on the analysis it is estimated that the light phase consists for 11 % of AEP. For the heavy phase it is concluded that almost no AEP is present and that for practical purposes the AEP content can be ignored.

4.3.1.2 Methyldiethanolamine (MDEA)

Graph 5 – MDEA concentration in the light (chemical) phase at various CO_2 pressures

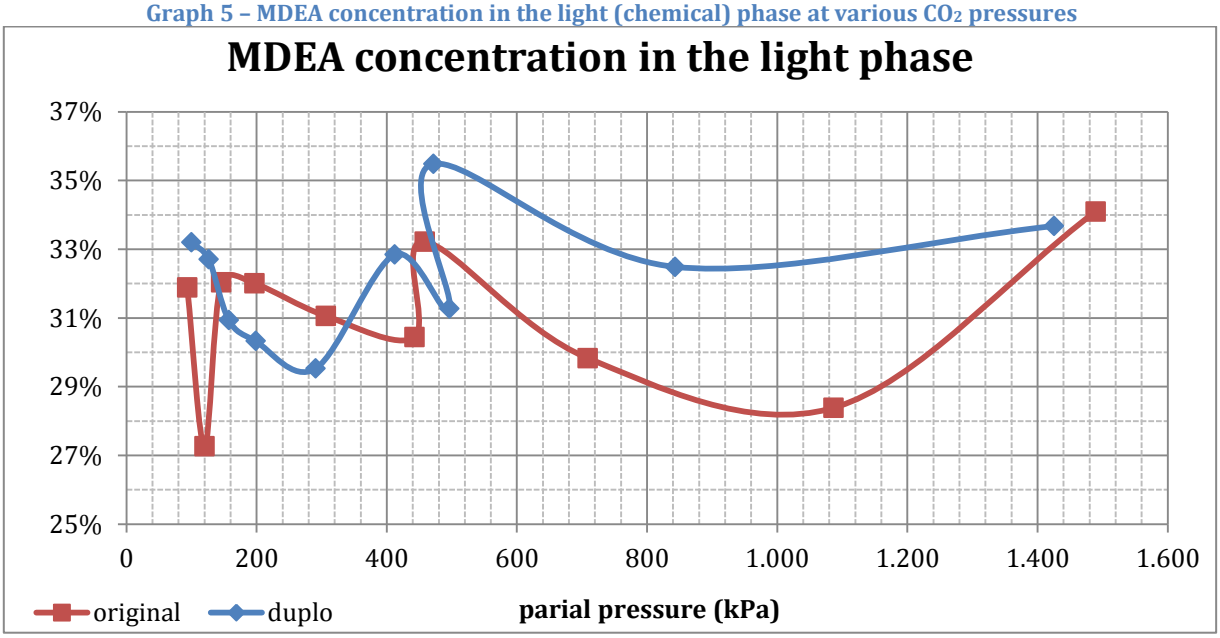

Graph 6 – MDEA concentration in the heavy (physical) phase at various CO_2 pressures

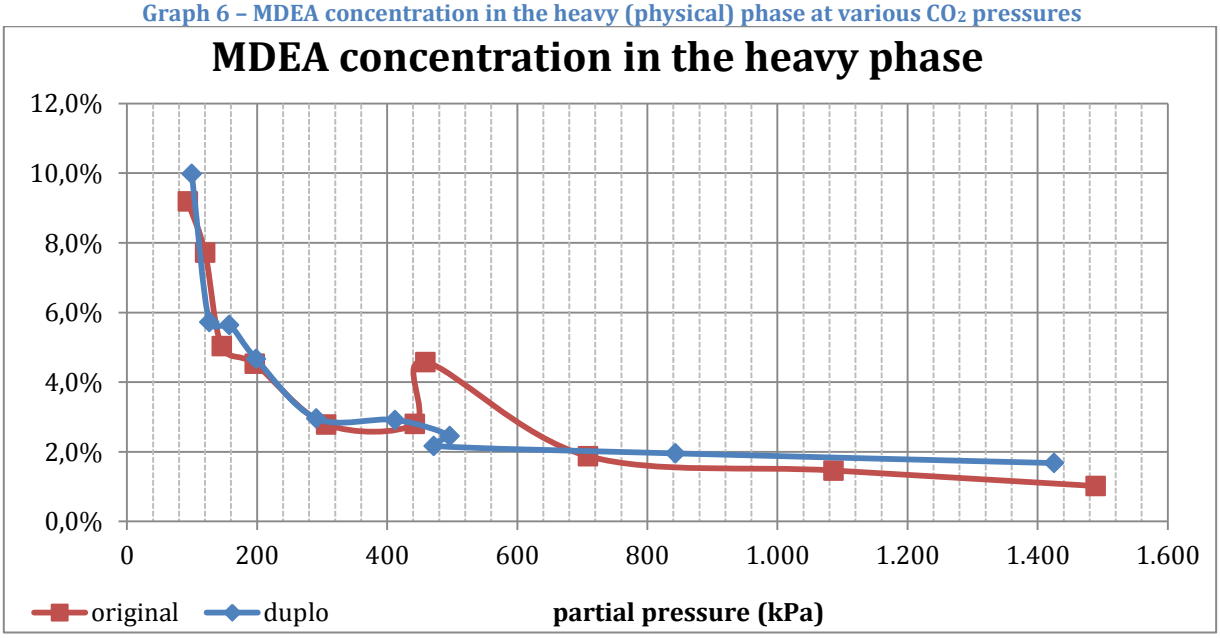

How the MDEA in the light and heavy phase changes can be seen in the two graphs on this page; graphs Graph 5 and Graph 6. The fact that the MDEA concentration in the light phase doesn't change while concentration in the heavy phase does might seem a violation of the law of mass conservation. However, this assumes that the total volume remains the same, which is not necessarily true. Furthermore, as the concentration of the other components in both phases are also changing, the law of mass conservation is not violated.

4.3.1.3 Sulfolane

Graph 7 – Sulfolane concentration in the light (chemical) phase at various CO_2 pressures

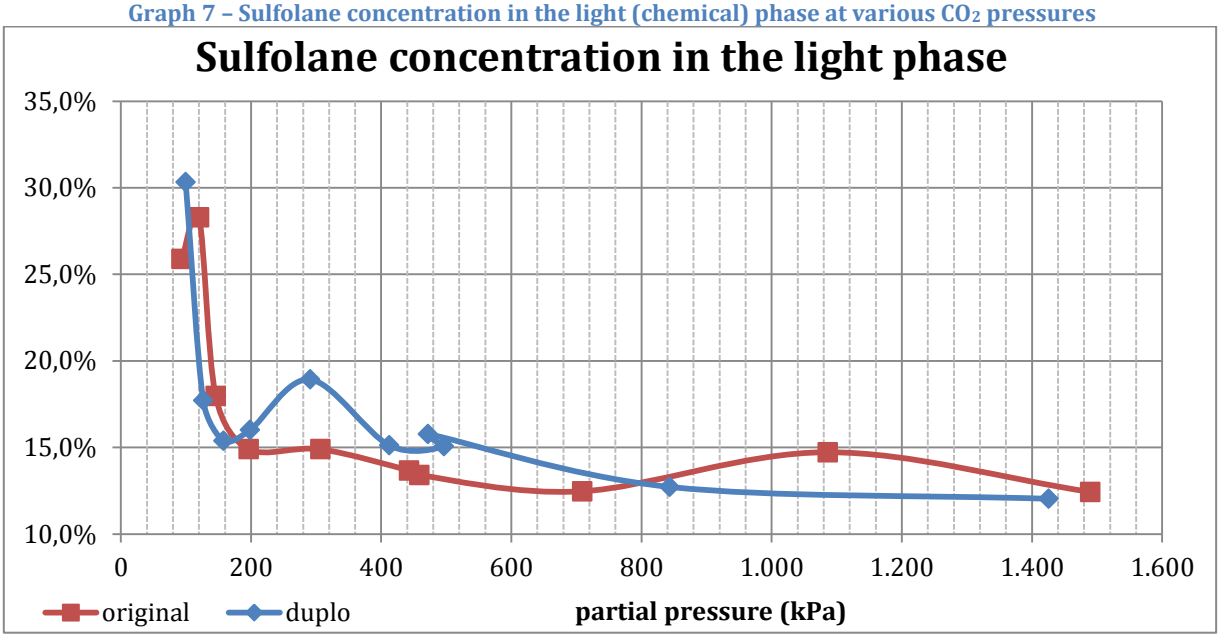

Graph 8 – Sulfolane concentration in the heavy (physical) phase at various CO_2 pressures

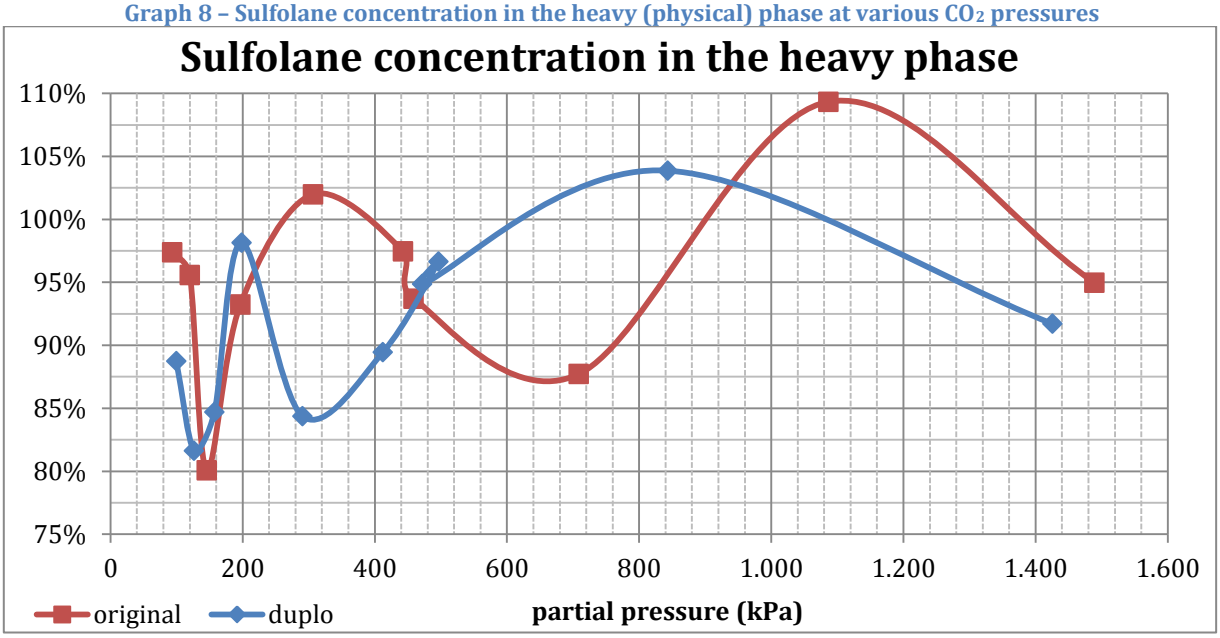

As can be seen from Graph 7, the sulfolane concentration in the light phase comes starts at ca. 30 % and stabilizes at 13 % at pressures above 200 kPa. However, the sulfolane concentration in the heavy phase doesn't follow such a clear trend. It is clear that the physical phase is predominantly sulfolane – that much can be concluded from Graph 8 and the other graphs. However, the concentrations are too scattered to be able to determine the concentration based on the graph.

Even though an accurate calibration line was made for sulfolane (r^2 of 0,9965), getting accurate and reproducible sulfolane concentration for the physical phase proved to be difficult. See for example Graph 9 which shows multiple analysis of heavy phase samples. The graph clearly shows that the reproducibility is low, since various concentrations are obtained when analysing a sample for the second or third time.

FTIR analysis has been used to cross reference these results proved to be unsuccessful, as these results did not produce realistic results. It was anticipated that FTIR analysis would work as sulfolane is the only compound containing two S=O bonds and thus should have a unique peak in the absorption spectra. However, for some reason this proved not to be the case.

Graph 9 - Reproducibility of the sulfolane concentration in the heavy phase using the GC. Each sample has been analysed in threefold as questions arose about the accuracy for the analysis.

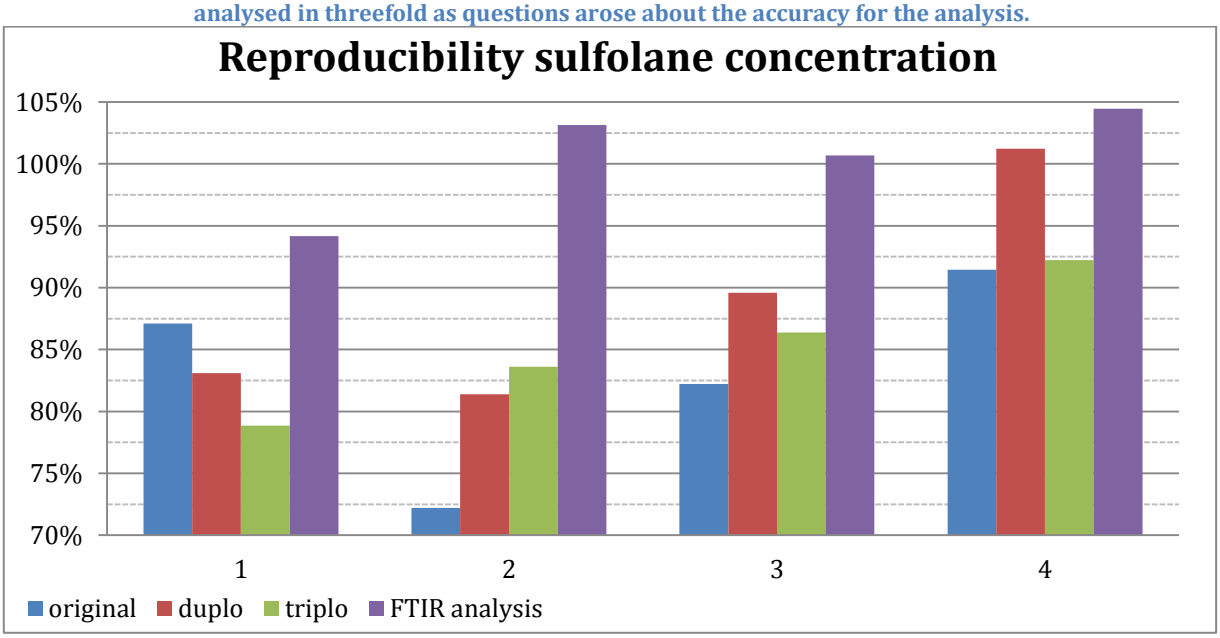

By heating the column to its limit (265 ^{0}C), cleaning the splitter with water and ethanol and removing the column's first 30 cm, it was – unsuccessfully – attempted to clean the column and to improve the results. Using a standard (either internal or external) was considered and rejected as these would not solve the problem. Ultimately, it was decided to use GC and initial calibration curves. As a result, the sulfolane concentration of the high phase should not be taken as an fixed number, but rather as an indication of the order of magnitude.

The difficulty is that there appear to be no problems when analysing the light phase (Graph 7). There is a clear trend for the sulfolane concentration in the light phase, despite one potential outlier. This seems to indicate that the column as such can be used and that the problem might be caused by something else and that replacing the column for another would thus not be necessary. However, during future research an alternative method of determining the sulfolane concentration needs to be used as the presented results are too scattered to use them when developing model or pilot plants. By using another column or analytical technique better results might be obtained even though that remains to be determined.

4.3.1.4 Water

Graph 10 – Water content of the light phase; based on Karl Fischer titrations

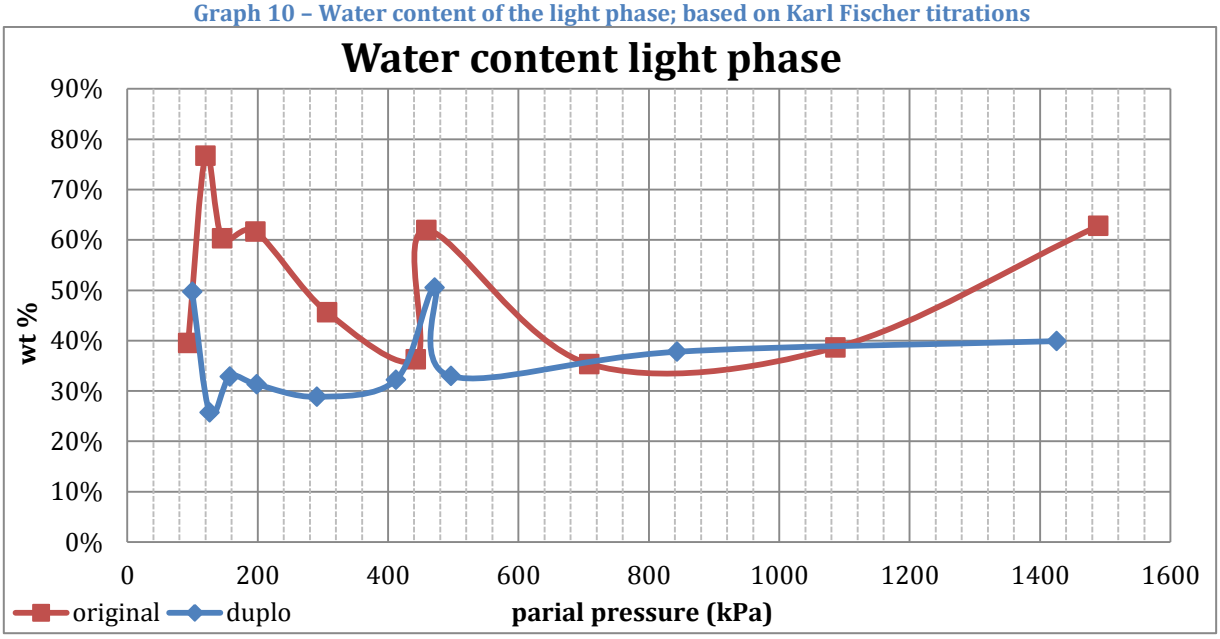

Graph 11 – Water content of the heavy phase; based on Karl Fischer titrations

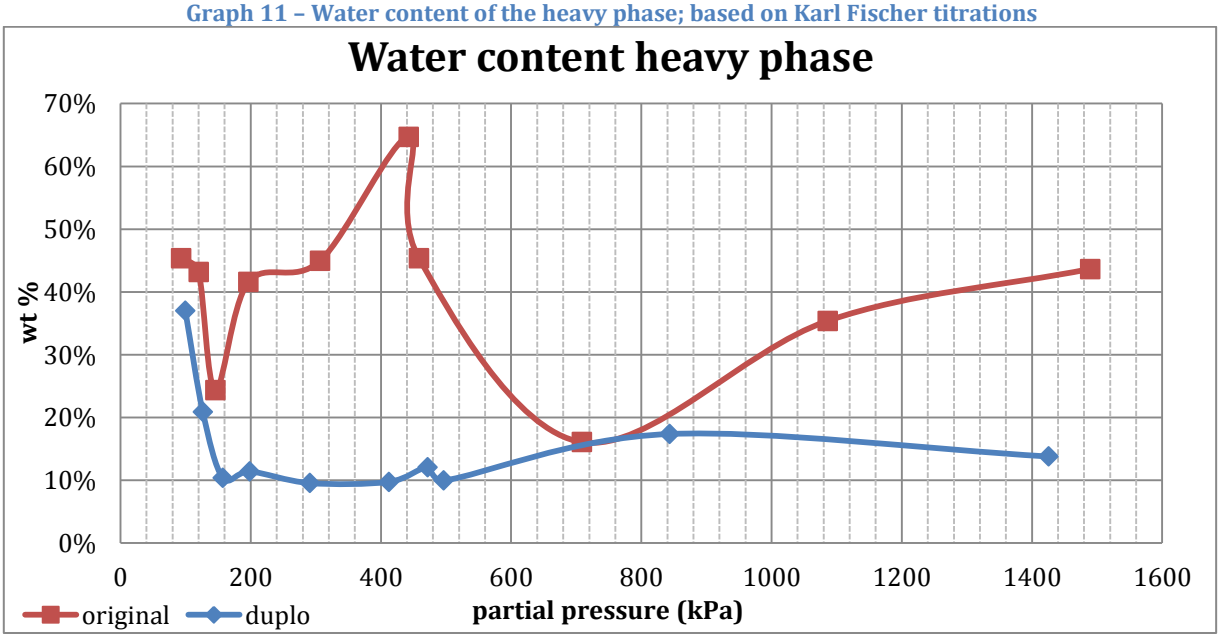

The results of the Karl Fischer titrations are shown in the graphs (10 and 11) above. As can be seen from the graphs, there doesn't appears to be a clear trend in the amount of water which can be found in either phase. This might be caused by faulty equipment. Testing standard test solutions gave readings conform their specifications which effectively eliminated faulty equipment as being the cause.

In addition to testing standard solution, various samples were analysed again in twofold. Another hypothesis was that the ethanol which was used might have caused the inaccuracies as ethanol can contain large amounts of water. However, high grade ethanol (≥ 99,99 % pure) was used to dilute the samples ca. 60 times, hence the amount of water is thought to be too small to cause the observed variances. To eliminate ethanol being the source, two samples were diluted while using high grade methanol (≥ 99,98 % pure)instead of ethanol. These results are in cooperated in the graph on the next page; Graph 12.

Also shown in the graph are the predicted water concentrations based on the mass balances. However, as in some of the samples the sulfolane concentration could not be determined accurately, some impossible results (e.g. sample 3) were obtained by this.

Graph 12 – Reproducibility of the water content when using the Karl Fischer titration while using both methanol and ethanol as the solvent. Also shown is the predicted water content which was based on the composition results of the GC analysis.

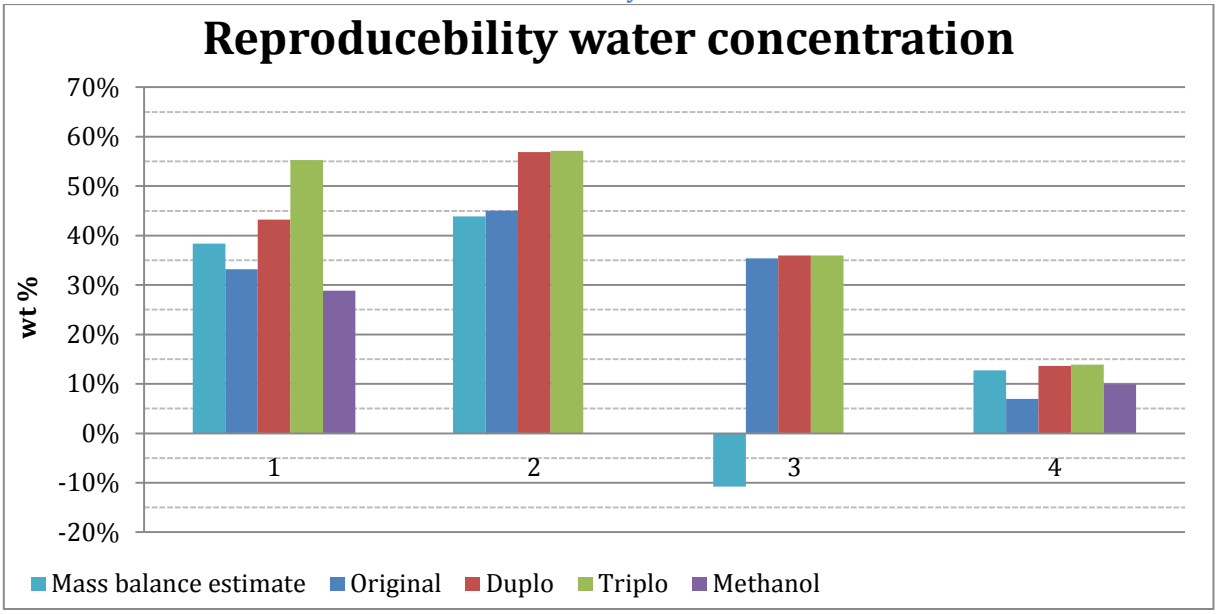

Graph 12 shows a number of interesting results. First of all: most of the duplo and triplo experiments appear to be consistent in terms of water content (excluding sample 1) even though large differences can exist between the original and duplo/triplo experiment (see e.g. samples 1 and 4). Furthermore, there is a considerable difference between using methanol and ethanol as a solvent, which is contrary to the assumption that there should be no difference between using methanol and ethanol.

Based on these results, the question rises whether Karl Fischer titrations are suitable to determine the water content of the used mixtures. Other methods to determine the water content do exist (e.g. the Dean Stark trap), but were unfortunately not available.

4.3.1.5 Mass balance of the blend and two phases

In order to verify the concentrations found by the GC analysis, mass balances were constructed to determine if the total mass of the components before and after loading is equal. Using the scale which has been added to the glass vessel (see also Figure 13) it can be estimate that the heavy phase is ca. 125 ml, whereas the light phase is approximately 450 ml. Using a 1:4 ratio between the two phases and the average composition of the two phases between 400 and 1.400 kPa, the following estimates were made.

Table 9 – Mass balance for AEP, MDEA and Sulfolane. The 2nd and 3rd column show the concentration is the light and heavy phase respectively. The 4th column shows the total of the phases while the 5th column is the composition of the unloaded blend.

	Heavy phase (%)	Light phase (%)	Total (%)	Blend (%)
AEP	0	11	9	10
MDEA	2	31	25	30
Sulfolane	94	13	29	35

Taking the assumptions that have been made into account (such as the 1:4 ratio between the heavy and the light phase), the numbers seem to be fairly close to the initial concentrations of ca. 30 wt% MDEA, 10 wt% AEP and 35 wt% sulfolane[14], even though the totals are somewhat lower which can be caused by the already mentioned uncertainties.

[14] For convenience, the blend was made while using a balance. As a result, slight variations in the composition can exist as not always exactly the same amount of absorbent was added to the blend. These small variations were not considered to be a problem, since it was anticipated that there will not be significant differences in terms of capture performances when using a blend with e.g. 9,8; 10 and/or 10,5 wt% AEP. However, the actual amount added was carefully recorded for future reference.

These results can be used to estimate the water content of each phase, as about 4 % water has to be present in the heavy phase and about 45 % water in the light phase. This yields an total water content of ca. 37 %, which is a major overestimation of the 25 % which was used in the blend. This overestimation is at least partly due to the assumptions in the mass balance. The results of the Karl Fischer titrations were not used as there was too much uncertainties in these results. However, should the estimates of the ratios in which the two phases be present become more accurate, the amount of water will be estimated more accurately.

Table 10 summarizes the composition of the phases at pressures between 000 and 400 kPa and between 400 and 1.400 kPa. The low pressure (100 – 400 kPa) composition was used for the VLE runs to determine the loading curves of the chemical and physical phase (see paragraph 4.3.2). Due to planning constrains it was not possible to use the high pressure phase composition for these experiments.

Table 10 - Summary of the phase composition at pressures between 100 and 1.400 kPa (between 0 and 100 kPa no phase slit was observed which is therefore not included).

	100 – 400 kPa		400 – 1.400 kPa	
	Heavy phase (wt %)	Light phase (wt %)	Heavy phase (wt %)	Light phase (wt %)
AEP	0,1	10,5	0	11
MDEA	4	30	2	31
Sulfolane	90	15	94	13
Water[15]	6	45	4	45

4.3.2 CO_2 loading of the blend and either phase

The loading of the blend as a whole was determined as a function of partial pressure. The result of this can be seen in Graph 13. The graph shows that the blend can achieve a loading of ca. 4,1 mole CO_2 per L of blend at a partial pressure of 1.500 kPa.

Graph 13 - CO2 loading of the blend (10 % AEP; 30 % MDEA; 35 % sulfolane; 25 % water) with partial pressures up to 1.500 kPa A

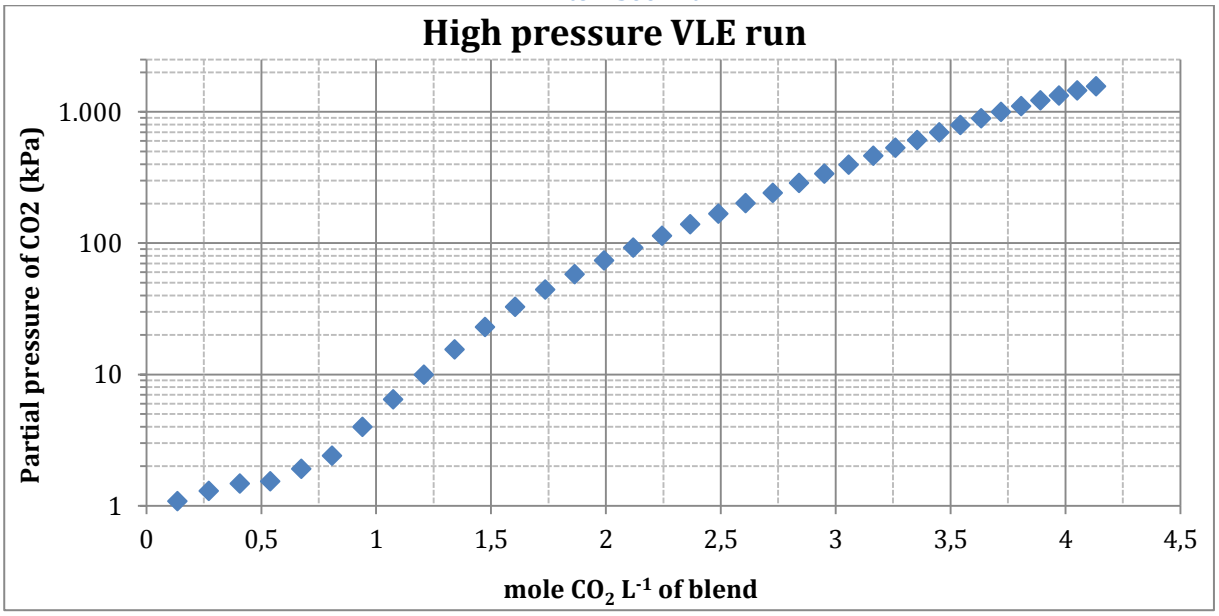

Note that there is no discontinuity in the loading curve can be observed as the system goes from one phase to two phases (this happens at the tipping point at ca. 100 kPa). This indicates that the act of two phases being formed has no influence on the performances of the blend.

4.3.2.1 Loading of the chemical phase

The loading of the chemical phase has been derived from the loading curves. Furthermore, the samples used for to determine the phase composition have been analysed with the FTIR to determine the

[15] The amount of water added was the amount needed to reach 100 wt.

loading. For the VLE test, only the chemical phase was tested, which was compiled based on the low pressure results (i.e. up to a pressure of 400 kPa), as presented in 4.3.1.

The compositions which are presented in Table 11 are based on the results of the composition analysis performed in paragraph 4.3.1 (see also Table 10). As can be seen, the amounts of AEP and MDEA are similar to the required composition. However, the sulfolane concentration of the chemical phase in this experiment is above the concentration found in the samples (18 vs. 15 %). The solvent was made gravimetrically, which explains the small overshoot of sulfolane and undershoot of water added. This was not considered to be a problem, since for the chemical phase the majority of the CO_2 is captured via the amines and small increase in sulfolane should not interfere with this.

Table 11 – Phase composition of the chemical phase for high pressure loading curves

	Chemical phase (wt %)
AEP	11,3
MDEA	31,1
Sulfolane	18,6
Water	39,1

The loading curve of the chemical phase and the results of the FTIR analysis are both shown in Graph 14[16]. The FTIR analysis was conducted on the same samples which were used to determine the phase composition. As a result, two complete sets of chemical phase samples (i.e. ranging from 0 to 1.500 kPa were available) have been analysed and are shown.

Graph 14 – Loading curve of the chemical phase (11,3 % AEP, 31,1 % MDEA, 18,6 % sulfolane, 39,1 % water); combined with the loading based on FTIR analysis of the samples which were used for phase compositions analysis.

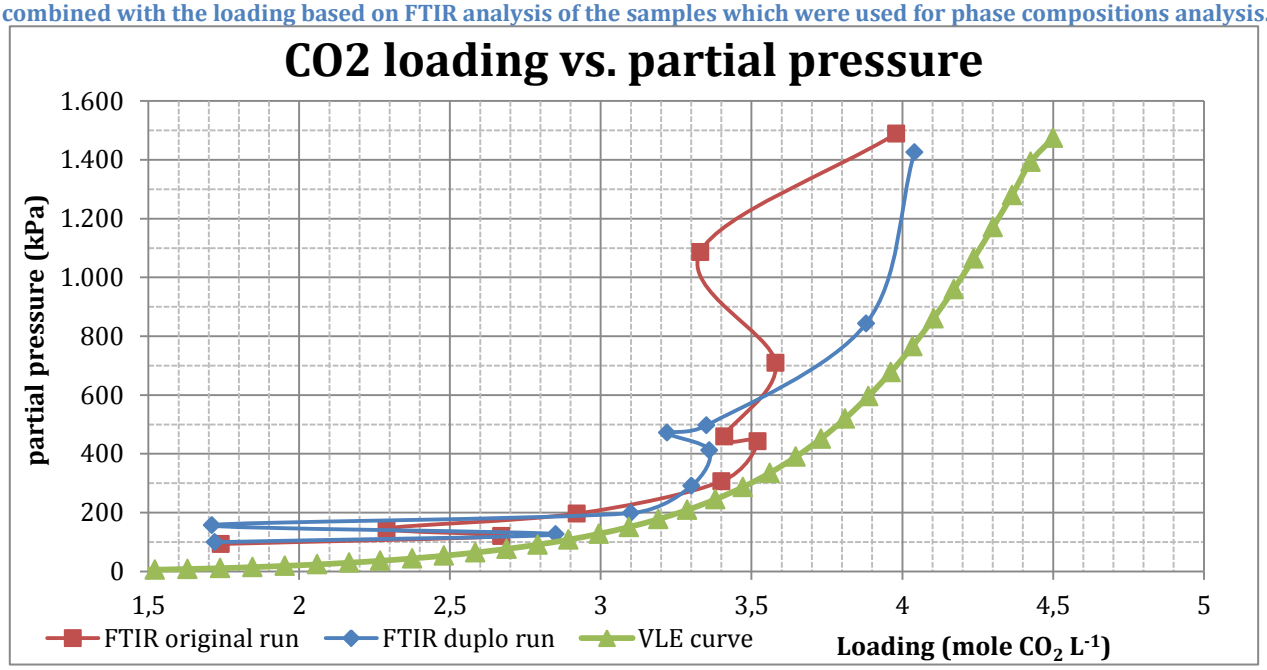

Even though the loading curve is considerably different from the FTIR analysis, some general comments can be made. Even though the FTIR analysis shows some unexpected behaviour around 180 kPa (see below) it follows the same general trend as the VLE curve. Furthermore, it was assumed that the CO_2 absorbed by the chemical phase would remain constant; whether being pressurized or not. Even though there is a slight decrease in loading at maximum pressure (4 mole CO_2 L^{-1} compared to 4,5 mole L^{-1}), the fast majority of the CO_2 remains absorbed.

The behaviour of the FTIR curves at pressures around 180 kPa is not clearly understood. Possibly the decrease in loading is effected by the two phases which have just been formed. Also, these points coincide with the same pressures at which peaks can be observed in e.g. the AEP concentrations (graphs Graph 3 and Graph 4) and the sulfolane concentration in the heavy phase (Graph 8). Further

[16] Appendix H shows the VLE curve but with pressure on the X-axis and loading on the Y-axis; which also nicely shows this behaviour.

analysis has to determine if these peaks are caused by the phases being formed or that another mechanism causes these peaks.

What is important when comparing the two graphs is to realize that during the VLE run (**Fout! Verwijzingsbron niet gevonden.**) no phase split has taken place as only the chemical phase was present. As a result, the loadings at low pressures are – probably – not easy to compare with the loadings of the samples. Furthermore, the uncertainty in the FTIR analysis are – on average – 0,1 mole/L, which has some influences on the overall result as well. Also, the FTIR has been calibrated between 0,19 and 3,45 mole/L. Hence the results outside this range – notably at the high concentrations – should be taken with care.

Even though the theoretical maximum amine loading of this phase is 3,66 mole/L[17], a higher loading is obtained. This might be due to physically absorbed CO_2. However, almost no gas was observed to flash when taking samples which implies that little CO_2 was physically absorbed. Another plausibility is that AEP absorbs more than 0,5 mole mole^{-1}, due to its structure of having multiple amine groups. Given sufficient time, the AEP might act as both a primary and tertiary amine and thus increase the chemical absorption of the solvent.

4.3.2.2 Loading of the physical phase

For the VLE runs of the heavy phase, a composition was used as described in Table 12. Compared to the desired composition (Table 10), a slightly higher amounts of amines were used which is again due to gravimetrically weighing the amines. These small increases in amine concentration are believed not to affect the loading significantly. Also, the amount of water in the phase is somewhat higher compared to the samples. This might slightly reduce the loading as sulfolane has a higher loading capacity that water.

Table 12 – Phase composition of the heavy phase for high pressure loading curves

	Heavy phase (%)
AEP	0,4
MDEA	2,9
Sulfolane	84,6
Water	12,1

The loading curve for the physical phase is similar to what is expected of a physical solvent. An almost linear relationship can be observed between the partial pressure and the loading with a maximum loading ca. 1,55 mole CO_2 per litre of heavy phase at a pressure of 1.500 kPa A; see Graph 15.

Graph 15 - Loading curve of the physical phase (0,4 % AEP, 2,9 % MDEA, 84,6 % sulfolane, 12,1 % water) at partial pressures up to 1.500 kPa A

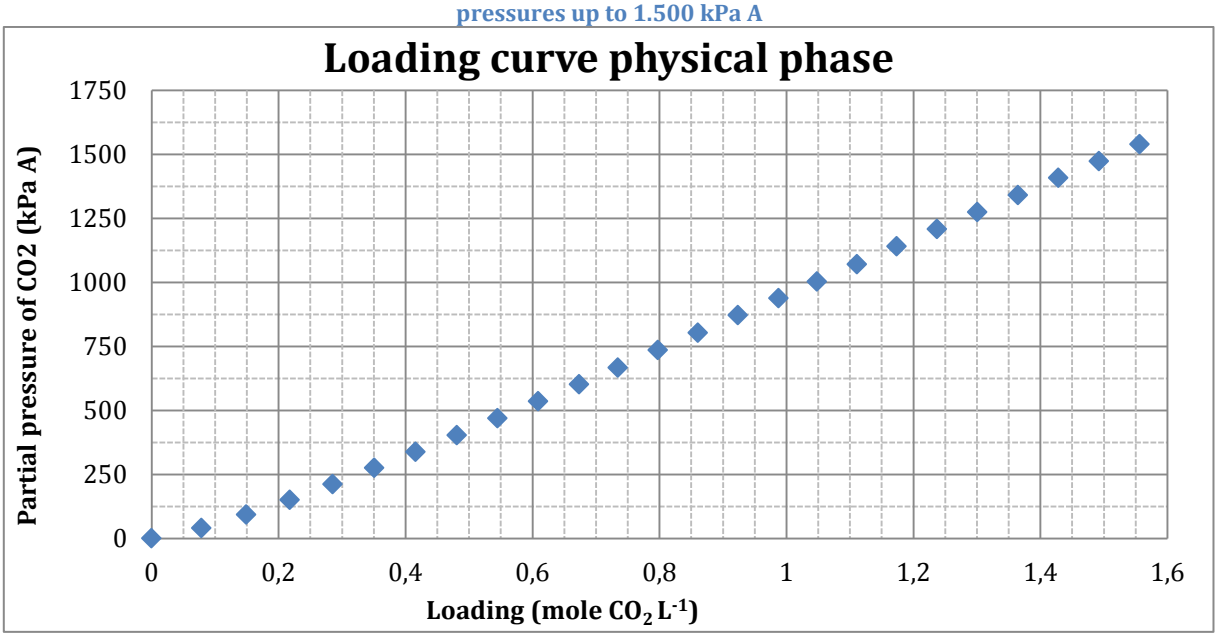

[17] Assuming an AEP loading of 0,5 mole mole^{-1}; 1 mole mole^{-1} MDEA loading and density of 1,21 gr/ml (see paragraph 4.3.3)

In contrast with the chemical phase, no FTIR analysis were conducted with the samples of the physical phase. As the heavy phase had flashed off already, hardly any CO_2 was present. For that reason, conducting a FTIR analysis was not considered to have much added value.

4.3.2.3 Carbon dioxide balance

Using a mass balance solely for the CO_2, the results of the VLE runs of the physical and chemical phase can be checked against the VLE run of the blend itself. Assuming again a 4:1 ratio between the chemical and physical phase (see also paragraph 4.3.1.5) and the loadings at 1.500 kPa, a total loading of 3,93 mole L^{-1} is obtained. This is close to the blend's loading which was obtained during the VLE experiment (Graph 13); see also Table 13. Given the small difference (5 %) between calculated and measured loading, the assumed 1:4 ratio between the chemical and physical phase seems to be accurate.

Table 13 - Carbon dioxide balance for both phases and the blend as a whole

	Physical phase (mole L^{-1})	Chemical phase (mole L^{-1})	Total (mole L^{-1})	Blend (mole L^{-1})
CO_2	1,55	4,52	3,93	4,13

4.3.3 Density of each phase

The density of the phases was initially determined using the sample tubes. However, despite various attempts and measure to ensure fully filled sample tubes, this technique did not work as the results were not consistent. For that reason the density was measured gravimetrically. The result of these experiments can be seen in Graph 16.

The fact that the experiments are conducted at atmospheric pressure can very clearly be seen in the density of the heavy phase. The density of this phase is roughly 1,25 gr/ml, which is slightly less than the density of sulfolane (1,26 gr/ml). Given that all the CO_2 is flashed of, this is not a surprise. The difference in density between the sulfolane and the observed density can be explained with the small amounts of water and MDEA being present. Since almost all CO_2 has flashed of, the physical phase's density while being pressurized is expected to be higher.

Graph 16 – Density of the two phases at various partial pressures

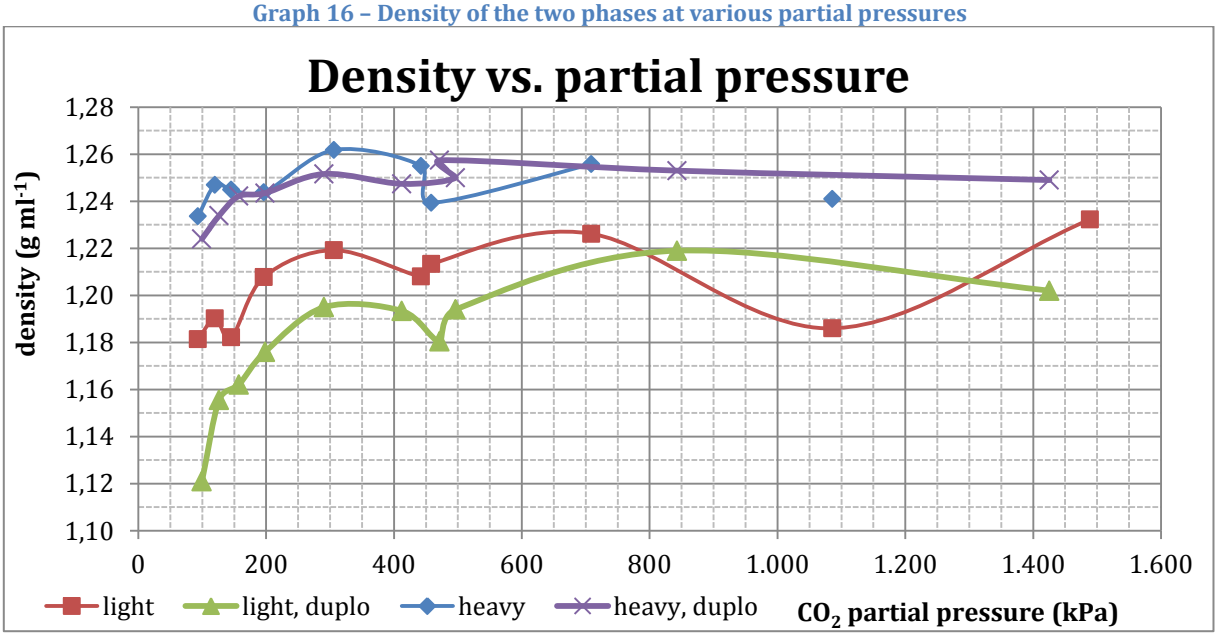

The density of the chemical phase is estimated to be ca. 1,21 gr/ml, which is ca. 3 % less compared to the physical phase. Even though this difference is believed to be larger when being loaded, it remains unclear if the density difference between the two phases is sufficient for easy and rapid separation in case of a full size capture plant.

As the sample tubes were not working as planned, pipettes were used to determine the loading of the – already flashed – physical phase. As a result, the relevance of the readings has been reduced significantly. Even though some errors might have been introduced by using the pipettes, these are

considered to be small compared to the effect of flashing of the solvent. What the cause is of the sample tubes method not working properly is unknown. The pressure in the VLE was stable when removing the sample tubes and – when being opened – some liquid came out of the second valve; both indicating the tubes being completely filled. Why this technique failed is not clear and is hopefully this can be solved for future measurements.

4.4 Heat of absorption

Having determined the composition of the chemical phase, the loading of the chemical phase was determined at various temperatures to determine the heat of absorption. This involved using the MAC at 40, 80 and 120 ^{0}C while using the composition as it is shown in Table 14. Again, this composition is not an exact copy of the results obtained during the composition analysis (table 11). However, based on the same arguments as the ones given in the previous paragraph, the composition was used.

Table 14 – Phase composition of the light phase for high temperature to determine the heat of absorption

	Light phase (%)
AEP	11,3
MDEA	32,3
Sulfolane	18,5
Water	37,9

Using the data from the MAC, the loading curves as shown in Graph 17 were obtained. As the MAC was used, all experiments were conducted to a maximum pressure of 450 kPa A max. Due to the evaporation of the water in the solvent during the 120 ^{0}C run, the maximum CO_2 partial pressure reached was less compared to the 40 and 80 ^{0}C experiments. These curves clearly show that increasing the temperature strips the CO_2 as – at constant pressure – the loading reduces significantly.

Graph 17 – Loading of the chemical solvent at various temperatures.

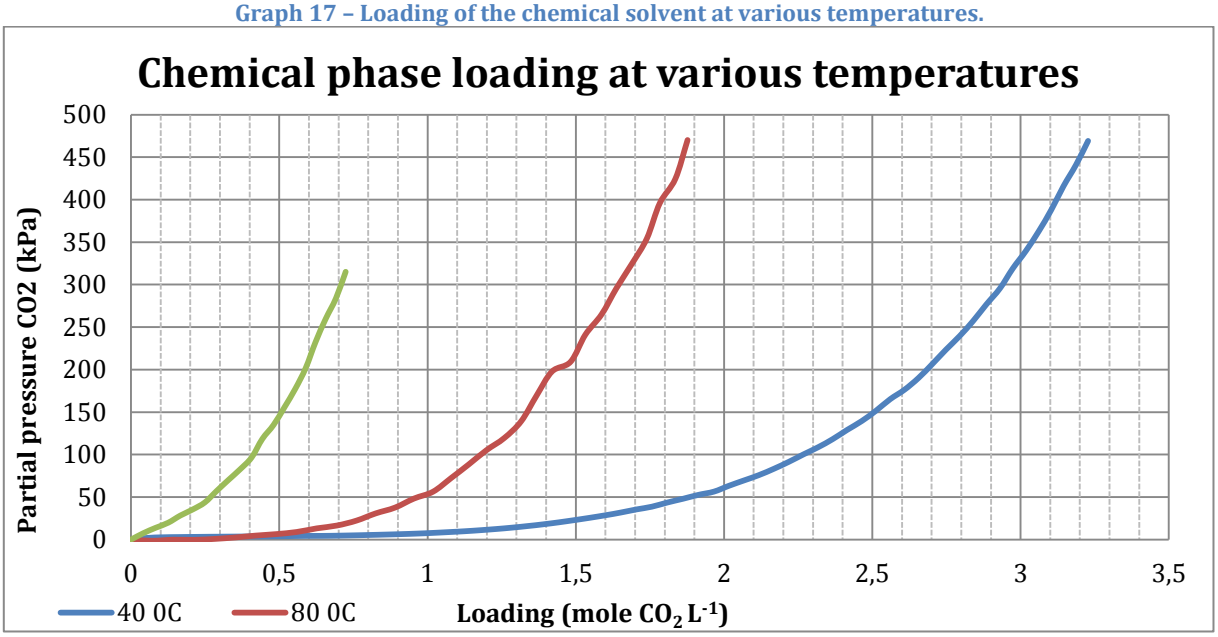

Using the Van ´t Hoff equation, the heat of absorption was calculated to be 44,5 kJ/mole[18]. Some of the calculated heats of absorption were ignored when calculating the average heat of absorption. These include heats of absorptions larger than -10 kJ mole^{-1} as these were considered as outliers.

The found result is slightly lower compared to other amines, which is slightly less than the numbers reported for MDEA (68). This is partly due to some of the physically absorbed CO_2. In the heat of absorption calculations there is no differentiation between the physically and chemically absorbed CO_2. As a result, the same amount of heat is used to regenerate a larger amount of CO_2 and, which makes comparison between various solvents troublesome. However, sulfolane is part of the light phase and thus it is inevitable that this influences the heat of absorption.

[18] Appendix I shows the data which is used to calculate this value.

Furthermore, only three loading curves are used in these calculations. Using additional curves (e.g. at 60 and 95 ^{0}C) would have make the results more accurate as more data would have been available. An additional advantage of having these curves would have been that the heat of absorption could also have been calculated while using higher loadings. Unfortunately these curves have not been obtained due to time constrains; which prevents the usage of these.

4.5 Energy consumption & comparison with aMDEA

At a temperature of 120 ^{0}C, the vapour pressure of the solvent is 150 kPa. Hence, the CO_2 pressure in the stripper will be 30 kPa. Using this information and the loading curves, the cyclic loadings were estimated at 3,84 mole per litre (light phase) and 0,62 mole (heavy phase). Using the 4:1 ratio between the light and heavy phase gives a total cyclic capacity of 3,20 mole per lire of blend. This means that 0,250 L of light phase and 0,063 L of heavy phase are required to capture one mole of CO_2.

The energy required to heat the light phase – which has a Cp value of 2,93 kJ kg^{-1} K^{-1} (69) (70) (71) and a density of 1,21 kg L^{-1} – 5 ^{0}C to reach the stripper temperature of 120 ^{0}C is estimated at 4,44 kJ per mole of CO_2. At this point, 38,31 kJ is required for the reaction to strip one mole of CO_2. Finally, to evaporate one mole of water, 32,54 kJ is required. Adding these numbers gives an energy consumption of 75,3 kJ per mole CO_2 which is equal to 1,71 GJ per ton CO_2. See also Graph 18 which clearly shows that the reaction energy and evaporating water are the majority of the energy consumption; heating makes only a small contribution.

Graph 18 – Energy consumption for the three thermal processes

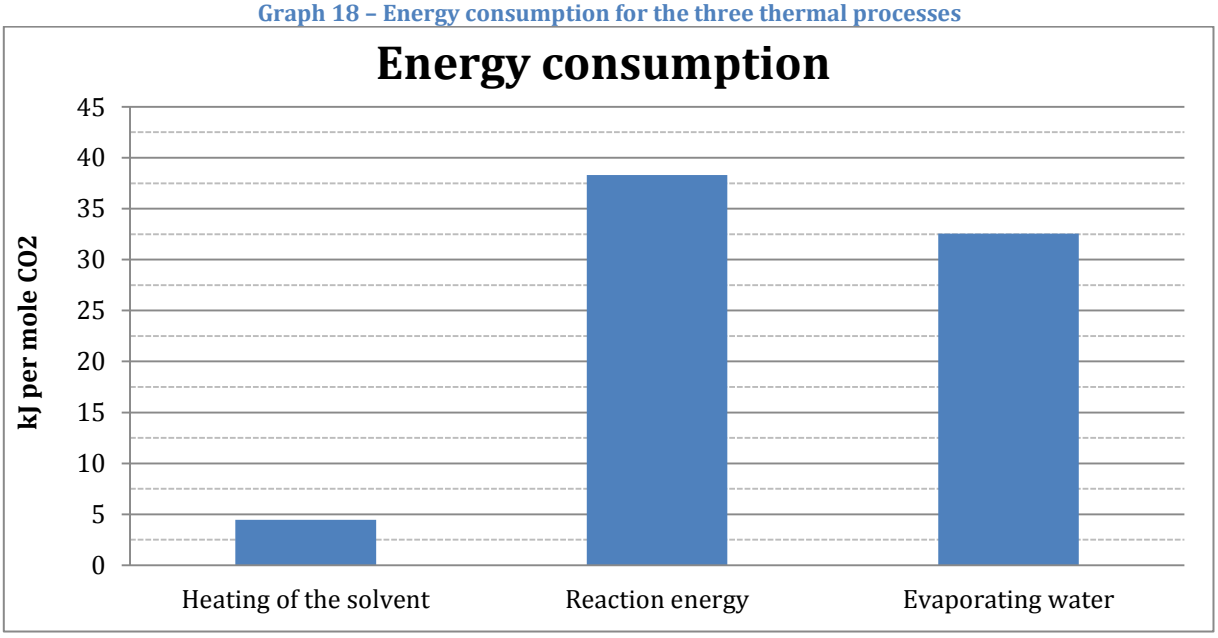

The natural gas coming out of the absorber is assumed to be at equilibrium with the lean chemical phase entering the column. In order to reach the stringent LNG specifications (50 ppm for CO_2) (72), this means that the CO_2 partial pressure has to be less than 0,3 kPa. The results of the chemical phase VLE run indicate that at this pressure (0,3 kPa) the equilibrium loading is ca. 1 mole per litre. Given that the lean loading is less, reaching the 50 ppm concentration should be possible.

However, it should be noted these concentrations and pressures are at the limit of which the VLE can accurately measure. This means that the 50 ppm objective is likely to be possible using this blend, even though the extent to which the energy requirements increase remains to be determined.

The blend which has been used can be compared with an aMDEA (activated MDEA) solution as the benchmark. aMDEA consists of a mixture of a secondary and tertiary amine and is commonly used for gas treatment. Comparison shows that the cyclic loading of the AEP/MDEA/sulfolane blend – at a CO_2 pressure of 700 kPa – is about 10 % higher than the aMDEA loading (3,19 mole L^{-1} for the blend and 2,88 mole L^{-1} (i.e. 0,625 mole mole^{-1}) for a 0,6M Pz/4M MDEA mixture (36).

In terms of energy consumption, the blend has better performances as well, as aMDEA has an energy consumption of 4,1 GJ per ton CO_2 to reach LNG specs (64). As the blend has a consumption of only 1,71 GJ ton^{-1}, this would be reduction of over 55%. Reducing the primary amine concentration might reduce the energy consumption even further, even though this might reduce the rate at which the CO_2 is absorbed. However, further research is needed in order to confirm the energy consumption of the blend, especially to reach the LNG specs which have been stated.

5 Conclusions

Based on the experimental results, a number of conclusions can be drawn. First of all, not all tested blends gave a split into two phases. The screening experiments give reason to believe that both sulfolane and MDEA have to be present for a phase split to occur. Which primary amines are additionally present don't seem to influence the phase split; even though this might influence properties such as density and loading. However, as only a limited number of blends have been tested, too little information is available for any further conclusions.

A blend consisting of 10 wt% AEP, 30 wt% MDEA, 35 % sulfolane and 25 % water was tested at pressures up to 1.500 kPa. These experiments aimed to determine the phase's loading and composition various CO_2 partial pressures. The blend reached a total loading of 4,1 mole L^{-1} at 1.500 kPa, with the two phase being formed in a 1:4 ratio (physical:chemical). At a partial pressure of ca. 100 kPa, the blend turned into a two phase system, with took less time to settle at higher partial pressures.

The physical (i.e. heavier) phase is predominantly made of sulfolane (ca. 94 wt%) with trace amounts of the other components being present. On the other hand, the chemical phase is much more of a mixture with AEP having a concentration of 11 %, 31 % MDEA, 13% sulfolane and the remaining 45 % water. However, there are uncertainties in especially the GC analysis and Karl Fischer titrations, which means that the results should be treated as an indication instead of a fixed number.

The obtained composition of each phase were used to obtain the loading curve of both phases (chemical and physical). These curves show that the loading of the chemical phase is significantly higher than the loading of the physical phase (4,5 vs. 1,52 mole L^{-1} at 1.500 kPa). The same holds for the density of the heavy phase, even though the difference between the phase is much less: only a 3 % density difference was observed between the two phases. However, due to flashing of the physical phase does this involved a loaded chemical and unloaded physical phase. Using other blends might increase this difference which should make separation of the two phases easier.

Furthermore, the cyclic loading and regeneration energy were determined and compared to a benchmark technologies (aMDEA). Based on the experiments, the blend – assuming the loading being equally distributed between the two phases – has a cyclic loading of ca. 3,20 mole L^{-1} (note: at 700 kPa), which is slightly above the aMDEA loading at that pressure (2,88 mole L^{-1}).

Finally, the heat of absorption was estimated to be 44,5 kJ mole $^{-1}$, which is slightly less than reported figures for e.g. MDEA. Also, the results indicate that the blend can be used for treating natural gas and to reach pipeline specs (50 ppm). The numbers indicate that this can be achieved while using less than 50% of the comparable aMDEA process. However, if those performance figures can be reached remains to be seen.

6 Recommendations

This thesis is almost entirely based on empirical evidence, with limited amount of theoretical data on amine used in carbon capture for support. This is the result of high pressure biphasic solvents being a novel development and that hence limited knowledge is available. As the scope of this research was to better understand the equilibrium behaviour, there are still a number of questions unanswered.

Given the exploring nature of this thesis, not knowing the driving force didn't cause any problems. However, one important questions which is still unanswered at this moment is what the exact requirements are for the (a?) blend to split into two phases. There is reason to believe that both MDEA and sulfolane have to be present for the split to occur. However, other combinations of amines and physical solvents might cause the same split. By determining and quantifying the mechanisms involved , the blend composition can be further optimized.

The blend can be optimized based on various criteria. . A blend of AEP, MDEA, sulfolane and water was used; which composition was based on previous experiments. By varying the concentration of the amines, it might be possible to lower the regeneration energy while keeping the cyclic loading the same. Also, solvent costs and reaction kinetics have not been considered in this thesis. Future reach focussing on these areas can be aimed at optimizing these, e.g. by using other amines such as piperazine.

In order to optimize the solvent, suitable analytical techniques have to be available to determine the composition of the phases. Even though the GC was capable of accurately determining most of the concentrations, the amount of sulfolane in the heavy phase could not be determined; just as the Karl Fischer titration not being able to determine the amount of water. Hence, alternative methods such as using another column, HPLC or GCMS analysis might be needed to improve the GC results, just as a Dean Start trap might be used for alternative water determinations.

Besides these recommendations which focus on the experiments which have been conducted, there are also a number of recommendations for the application of this technique. For example, this thesis has not taken H_2S removal into account, even though for acid gas fields H_2S removal can be just as important as CO_2 removal. Since no experiments were conducted with H_2S, nothing is known about the capabilities of absorbing H_2S or the selectivity for either H_2S or CO_2. However, for a Claus unit to successfully process the obtained acid gas, the H_2S concentration has to be within certain limits. Future research has to show whether this technique can be used in combination with a Claus unit.

Also, the absorber design which has been used (feeding both the regenerated physical and chemical phase at the top of the absorption column) during the energetic analysis can be improved significantly. Feeding the lean solvents at various points to the absorber, using a split feed for the stripper and/or having tapping the rich solvents at various points in the absorber column might further reduce the energy consumption of this technique. It is believed that by clever designing the energy requirements of this process can be brought down even further.

An interesting side track might be to only use the chemical phase as a solvent,. As said, the density difference between the two phases is very small while the cyclic loading of the light phase is high. By taking the heavy phase out of the design, the process design will become less difficult and (thus) less expensive. Doing so would cause an energy penalty for the plant as more energy is required to regenerate the solvent. However, it might be an interesting option to consider.

7 Works sited

1. **Project Smart Explorer.** Oil and gas prices do not stop Shell and ADNOC in UAE Bab sour gas. [Online] 2B1st Consulting, 23rd January 2015. [Cited: 16th June 2015.] http://www.2b1stconsulting.com/oil-and-gas-prices-do-not-stop-shell-and-adnoc-in-uae-bab-sour-gas/?doing_wp_cron=1434438468.8000450134277343750000.

2. **Intergovernmental Panel on Climate Change.** *Renewable Energy Sources and Climate - Special Report of the Intergovernmental.* New York, USA : Cambridge University Press, 2012. p. 982.

3. **World Energy council.** *Water for Energy.* London, UK : World Energy Counsil, 2010. 978-0-946121-10-6.

4. *Hysweet Technology: A Major Progress in Sour Gas Processing.* **Zhao, Jing, et al.** Abu Dhabi, UAE : s.n., 2012. Abu Dhabi International Petroleum Exhibition & Conference. pp. 1 - 10.

5. **U.S. Energy Information Administration.** Global natural gas consumption doubled from 1980 to 2010. *Today in Energy.* [Online] U.S. Energy Information Administration, 12th April 2012. [Cited: 2nd February 2015.] http://www.eia.gov/todayinenergy/detail.cfm?id=5810.

6. *Worldwide development potential for sour gas.* **Burgers, W. F. J., et al.** 4, Houston, USA : Elsevier, 2011, Energy Procedia, pp. 2178 - 2184.

7. **Huo, Da.** The Global Sour Gas Problem. *Standford Energy Club.* [Online] 26th November 2012. [Cited: 21st May 2015.] http://energyclub.stanford.edu/journalitem/the-global-sour-gas-problem/.

8. **Schlumberger.** Enhanced oil recovery. *Oilfield Glossary.* [Online] Schlumberger, 2015. [Cited: 24th February 2015.] http://www.glossary.oilfield.slb.com/en/Disciplines/Enhanced-Oil-Recovery.aspx.

9. **Kohl, Arthur and Nielsen, Richard.** *Gas Purification.* Houston, Texas (USA) : Gulf Publising Company, 1997. 0-88415-200-0.

10. **Royal Dutch Shell.** Sour gas processing - recent project experiences demonstrate the effectiveness of integrated solutions. [Online] [Cited: 26th June 2015.] http://www.shell.com/content/dam/shell/static/globalsolutions/downloads/media-centre/industry-commentary/sour-gas-processing.pdf.

11. **Kemenade, van, H. P.; Brouwers, J. J. H. and Rijke, de, S. J. M.** Comparing the Volume and Energy Consumption of Sour-Gas Cleaning by Condensed Rotational Separation and Amine Treatments. *Energy Technology.* 2013, Vol. 1, 7, pp. 392 - 394.

12. *CO2 capture and separation technologies for end-of-pipe applications - A review.* **Olajire, Abass.** 35, Ogbomoso, Nigeria : Elsevier, 8th April 2010, Energy, pp. 2610 - 2628.

13. **Maddox, Robert and Morgan, John.** *Gas Conditioning and Processing - Volume 4: Gas Treating and Sulfur Recovery.* Norman : Campbell Petroleum Series, 2008. pp. 5 - 6. 0-9703449-3-7.

14. **Yu, Cheng-Hsiu, Huang; Chih-Hung and Tan, Chung-Sung.** A review of CO2 catpure by absorption and adsorption. *Aerosol and air quality research.* 2012, Vol. 12, pp. 745 - 769.

15. **Fouad, Wael A. and Berrouk, Abdallah S.** Using mixed tertiary amines for gas sweetening energy requirement reduction. *Journal of Natural Gas Science and Engineering.* 2013, Vol. 11, pp. 12 - 17.

16. **Adeosun, Adewale, et al.** Absorption of CO2 by amines blend solutions: an experimental evaluation. *International journal of engineering and science.* 2013, Vol. 3, 9, pp. 12 - 23.

17. **Yeo, Zee Ying, et al.** Conventional processes and membrane technology for carbon dioxide rmoval from natural gas: a review. *Jornal of Natural Gas Chemistry.* 2013, Vol. 21, 3, pp. 282 -298.

18. **Burr, Barry and Lyddon, Lili.** A comparison of physical solvents for acid gas removal. [Online] 2008. [Cited: 2th February 2015.] http://www.bre.com/portals/0/technicalarticles/A%20Comparison%20of%20Physical%20Solvents%20for%20Acid%20Gas%20Removal%20REVISED.pdf.

19. *The removal of CO2 and N2 from natural gas: a review of conventional and emerging process technologies.* **Rufford, T. E., et al.** Crawley, Australia : s.n., 2012, Journal of Petroleum Science and Engineering, pp. 123 - 154.

20. *Selection of new absorbents for carbon dioxide capture.* **Ma'mun, Sholeh, et al.** 48, Trondheim, Norway : Elsevier, 2006, Energy Conversion & Management, pp. 251 - 258.

21. *A Review of CO2 Capture by Absorption and Adsorption.* **Cheng-Hsiu, Yu; Chih-Hung, Huang and Shung-Sung, Tan.** 2012, Aerosol and Air Quality Research, pp. 745 - 769.

22. *Absorption rates and CO2 solubility in new pierazine blends.* **Li, Le, et al.** 37, Austin, Texas : Elsevier, 2013, Energy Procedia, pp. 370 - 385.

23. *Pilot-scale exeriments for post-combustion CO2 capture from gas fired power plants with a novel solvent.* **Esmaeili, Hamid and Roozbehani, Behrooz.** 30, Abadan, Iran : Elsevier, 2014, International Journal of Greenhouse Gas Control, pp. 212 - 215.

24. *Economic assessment of novel amine based CO2 capture technologies integrated in power plants based on European benchmarking task force methoology.* **Manzolini, G., et al.** Milan, Italy : Elsevier, 2015, Applied Energy, Vol. 138, pp. 546 - 558.

25. **Monteiro, Juliana G. M.-S., et al.** VLE data and modelling of aqueous N,N-diethylethanolamine (DEEA) solutions. *International Journal of Greenhouse Gas Control.* 2013, Vol. 19, pp. 432 - 440.

26. *The DMX process: an original solution for lowering the costs of post-combustion carbon capture.* **Raynal, Ludovic, et al.** 4, Salaize, France; Rueil-Malmaison, France : Elsevier, 2011, Energy Procedia, pp. 779 - 786.

27. *Overall process analysis and optimisation for CO2 capture from coal fired power plants based on phase change solvents froming two liquid phases.* **Liebenthal, Ulrich, et al.** 37, Hamburg, Germany; Trondheim, Norway : Elsevier, 2013, Energy Procedia, pp. 1844 - 1854.

28. *Development of an energy-efficient CO2 capture process using thermomorphic biphasic solvents.* **Zhang, Jiafei, et al.** 37, s.l. : Elsevier, 2013, Energy Procedia, pp. 1254 - 1261.

29. **Energy Information Administration.** *Natural Gas Processing: The Crucial Link Between Natural Gas Production and Its Transportation to Market.* 2006.

30. **Sanchez Fernandez, Eva.** *Novel process designs to improve the efficiency of postcombustion carbon dioxide capture.* Delft, The Netherlands : Ipskamp Drukkers BV, 2013.

31. **Wikipedia.** Primary amine 2D general. *Wikipedia.* [Online] 8th July 2011. [Cited: 16th April 2015.] https://en.wikipedia.org/wiki/Amine#/media/File:Primary-amine-2D-general.svg.

32. —. Secondary amine 2D general. *Wikipedia.* [Online] 8th July 2011. [Cited: 16th April 2015.] https://en.wikipedia.org/wiki/Amine#/media/File:Secondary-amine-2D-general.svg.

33. **Mazari, Shaukat A., et al.** An overview of solvent management and emissions of amine-based CO2 capture technology. *International journal of greenhouse gas controle.* 2015, Vol. 34, pp. 129 - 140.

34. **Wikipedia.** Amine 2D general. *Wikipedia.* [Online] 8th July 2011. [Cited: 16th April 2015.] https://en.wikipedia.org/wiki/Amine#/media/File:Amine-2D-general.svg.

35. **Notz, R., et al.** Selection and pilot plant tests of new absorbents for post-combustion carbon dioxide capture. *Chemical engineering research and design.* 2007, Vol. 85, 4, pp. 510 - 515.

36. **Bishnoi, Sanjay and Rochelle, Gary T.** Absorption of Carbon Dioxide in Aqueous Piperazine/Methyldiethanolamine. *American Institute of Chemical Engineers Journal.* 2002, Vol. 48, pp. 2788 - 2799.

37. **Svensson, Helena; Hulteberg, Christian and Karlsson, Hans T.** Heat of absorption of CO2 in aqueous solutions of DEEA, MAPA and their mixture. *Energy Procedia.* 2013, Vol. 17, pp. 89 - 98.

38. **Tagliabue, Marco, et al.** Natural gas treating by selective adsorption: Material science and chemical engineering interplay. *Chemical Engineering Journal.* 2009, Vol. 155, pp. 553 - 566.

39. **Brúder, Peter, et al.** Natural gas treating by selective adsorption: Material science and chemical engineering interplay. *Chemical Engineering Science.* 2011, Vol. 66, pp. 6193 - 6198.

40. *CO2 absortion in biphasic solvents with enhanced low temperature solvent regeneration.* **Zhang, Jiafei, et al.** 4, Dortmund, Germany : Elsevier, 2011, Energy Procedia.

41. **Gervasi, Julien; Dubois, Lionel and Thomas, Diane.** Screening tests of new hybrid solvents for the post-combustion CO2 capture process by chemical absorption. *Energy Procedia.* 2014, Vol. 63, pp. 1854 - 1862.

42. **Porcheron, Fabien, et al.** High throughput screening of amine thermodynamic properties applied to post-combustion CO2 caputre process evaluation. *Energy Procedia.* 2011, Vol. 4, pp. 15 - 22.

43. **Just, Paul-Emmanuel.** Advances in the development of CO2 capture solvents. *Energy Procedia.* 2013, Vol. 37, pp. 314 - 324.

44. **Aronu, Ugochukwu E., et al.** Solvent selection for carbon dioxide absorption. *Energy Procedia.* 2009, Vol. 1, 1, pp. 1051 - 1057.

45. **Chowdhury, Firoz A., et al.** Development of novel tertiary amine absorbents for CO2 capture. *Energy Procedia.* 2009, Vol. 1, 1, pp. 1241 - 1248.

46. **Oexmann, Jochen and Kather, Alfons.** Minimising the regeneration heat duty of post-combustion CO2 capture by wet chemical absorption: the miguided focus on low heat of absorption solvents. *International Journal of Greenhouse Gas Controll.* 2010, Vol. 4, 1, pp. 36 - 43.

47. **Murrita-Guevara, Florentino; Rebolledo-Libreros, Esther and Trejo, Arturo.** Gas solubility of carbon dioxide and hydrogen sulfide in mixtures of sulfolane with monoethanolamine. *Fluid Phase Equilibria.* 1993, Vol. 86, pp. 225 - 231.

48. **Hilliard, Marcus Douglas.** *A Predictive Thermodynamic Model for an Aqueous Blend of Potassium Carbonate, Piperazine, and Monoethanolamine for Carbon Dioxide Capture from Flue Gas.* Austing, Texas (USA) : s.n., 2008.

49. **Kim, Inna; Anders, Karl and Mejdell, Thor.** Heat of Absorption of CO2 with Aqueous Solutions of MEA: New Experimental Data. *Energy Procedia.* 2014, Vol. 63, pp. 1446 - 1455.

50. **Freeman, Stephanie A., et al.** Carbon dioxide capture with concentrated, aqueous piperazine. *International Journal of Greenhouse control.* 2009, Vol. 4, 2, pp. 119 - 124.

51. **Adeosun, Adewale, et al.** Absorption of CO2 by amines blends solution: an experimental evaluation. *International Journal of Engineering and Science.* 2013, Vol. 3, 9, pp. 12 - 23.

52. **Geers, Leon F. G., et al.** Development of an Online Monitoring Method of a CO 2 Capture Process. *Industrial & Engineering Chemistry Research.* 2011, Vol. 50, 15, pp. 9175 - 9180.

53. **Diab, Farah, et al.** Quantitative analysis of the liquid phase by FT-IR spectroscopy in the system CO2/diethanolamine (DEA)/H2O. *Fluid Phase Equilibria.* 2012, Vol. 325, pp. 90 - 99.

54. **Silva, Sandra D., et al.** Application of FTIR-ATR to Moscatel dessert wines for prediction of total phenolic and flavonoid contents and antioxidant capacity. *Food Chemistry.* 2014, Vol. 150, pp. 489 - 493.

55. **Wilcox, Jennifer.** *Carbon Capture.* Standord, California (USA) : Springer, 2012. 978-1-4614-2214-3.

56. **Sanchez-Fernandez, Eva, et al.** Precipitating amino acid solvents for CO2 capture. Opportunities to reduce costs in Post combustion capture. *Energy Procedia.* 2014, Vol. 63, pp. 727 - 738.

57. *Pilot Plant Experiments for Post Combustion Carbon Dioxie Capture by Reactive Absortion with Novel Solvents.* **Mangalapaly, Hari Prasad and Hasse, Hans.** 4, Kaiserslautern, Germany : Elsevier, 2011, Energy Procedia, pp. 1 - 8.

58. *Use of Selexol process in coke gasification to ammonia projects.* **Breckenridge, William, et al.** Norman, Oklahoma (USA) : s.n., 2000.

59. **Mettler Toledo.** *Good Titration Practise in Karl Fischer Titrations.*

60. **Sigma-Aldrich.** HYDRANAL is going green ... Karl Fischer titration with ethanol-based reagents. *HYDRANAL®-E Types.* [Online] [Cited: 16th June 2015.] http://www.sigmaaldrich.com/analytical-chromatography/titration/hydranal/hydranal-reg-e-types.html.

61. **Geankoplis, Christie John.** *Transport processes and Separation process principles.* Upper Saddle River, New Jersey (USA) : Prentice Hall, 2008. 0-13-101367-X.

62. **Sulzer Chemtech.** Liquid-Liquid separation technology. *Sulzer Chemtech.* [Online] [Cited: 26th June 2015.] http://www.sulzer.com/nl/-/media/Documents/ProductsAndServices/Separation_Technology/Coalescers/Brochures/Liquid_Liquid_Separation_Technology.pdf.

63. **Atkins, Peter and Paula, de, Julio.** *Atkins' Physical Chemistry.* s.l. : Oxford University Press, 2009. 978-0-19-954337-3.

64. *Multi-criteria analyses of two solvent and one low-temperature concepts for acid gas removal from natural gas.* **Roussanaly, Simon; Anantharaman, Rahul and Lindqvist, Karl.** 20, 2014, Journal of Natural Gas Science and Engineering, pp. 38 - 49.

65. **Zoannou, Kali-Stella; Sapsford, Devin J. and Griffiths, Anthony J.** Thermal degradation of monoethanolamine and its effect on CO2 capture capacity. *International Journal of Greenhouse Gas control.* 2013, Vol. 17, pp. 423 - 430.

66. **Davis, Jason Daniel.** *Thermal degradation of Aqueous Amines Used for Carbon Dioxide Capture.* Austin, Texas (USA) : s.n., 2009.

67. **Du, Yang, et al.** Aqueous piperazine/N-(2-aminoethyl) piperazine for CO2 capture. *Energy Procedia.* 2013, Vol. 37, pp. 1621 - 1638.

68. *Heat of absorption of carbon dioxide (CO2) into aqueous N- methyldiethanolamine (MDEA) and N,N-dimethylmonoethanolamine (DMMEA).* **Jonassen, Oystein; Kim, Inna and Svendsen, Hallvard F.** 2014, Energy Procedia, pp. 1890 - 1902.

69. **Dow Chemical Company.** *Aminoethylpiperazine - product information.* Midland, Michigan (USA) : The Dow Chemical Company, 2001.

70. **Maham, Yadollah, et al.** Molar heat capacities of alkanolamines from 299,1 to 397,8 K. *Journal of the Chemical Society - Faraday Transactions.* 1997, Vol. 93, 9, pp. 1747 - 1750.

71. **Castagnolo, Maurizio, et al.** Volumes and heat capacities of binary liquid mixuters of water-sulfolane and water-hexamethylphosphotriamide. *Thermochimica Acta.* 1981, Vol. 44, 1, pp. 67 - 76.

72. *Low-temperature CO2 removal from natural gas.* **Berstad, David; Neska, Petter and Anantharaman, Rahul .** 26, 2012, Energy Procedia, pp. 41 - 48.

73. **Laan, R, van der.** *Toegepast Fasenleer.* Houten, The Netherlands : Bohn Stafleu van Loghum, 2000. pp. 51 - 54. 90-313-3412-X.

74. **Dang, Hongyi and Rochelle, Gary T.** Absorption Rate and Solubility in Monoethanolamine/Piperazine/Water. *Separation Science and Technology.* 2003, Vol. 38, 2, pp. 337 - 357.

75. **Abu-Zahra, Mohammad R.M., et al.** CO2 capture from power plants Part I. A parametric study of the technical performance based on monoethanolamine. *International journal of greenhouse gas control.* 2007, Vol. 1, pp. 37 - 46.

76. **Svensson, Helena, Hulteberg, Christian and Karlsson, Hans T.** Precipitation of AMP carbamate in CO2 absorption process. *Energy Procedia.* 2014, Vol. 63, pp. 750 -757.

8 Appendices

Appendix A – Chemical and equipment used

Chemicals:

Table 15 – Amines & physical solvents used for making the blends

Chemical	Supplier	Grade
AEP	Acros Organics	99 %
AMP	Acros Organics	99 %
DEA	Aldrich Chemistry	99 %
DEEA	Aldrich Chemistry	≥ 99,5 %
DMCA	Aldrich Chemistry	99 %
MDEA	Aldrich Chemistry	≥ 99 %
MEA	Aldrich Chemistry	≥ 99 %
Pz	Sigma Aldrich	99 %
Sulfolane	Aldrich Chemistry	99 %
TDG	Fluka Analytical	≥ 95 %

Table 16 - Other chemicals used during the course of this thesis

Chemical	Supplier	Grade
Phosphoric Acid	Sigma Aldrich	≥ 85 %
Ethanol	Fischer Chemical	> 99,99 %
Methanol	Biosolve BV	≥ 99,98 %
CO_2	Air Liquide	> 99,5 %
N_2	Air Liquide	> 99,5 %

Equipment:

Density measurement:
Manufacture: Anton Paar
Model: DMA 4500 Density Meter

Gas Chromatograph:
Manufacture: Thermo Scientific
Model: Focus GC
Column: Restek fused silica; 30 meter; 0,53 mm ID, 5 µm DF

FTIR:
Manufacture: Thermo Electron Corporation
Model: Nicolet 6700 FT-IR

Karl Fischer titration:
Manufacture: Mettler Toledo
Model: C20 Coulometric KF Titrator
Working solution: Hydranal®
Tested standard: Hydranal® water standard 1.0 (0,1 wt% water)

Gas analyser (Phosphoric acid set-up):
Manufacture: Rosemount
Model: Binos 100 2M

Appendix B – gas chromatograph calibration

The samples were diluted by different amounts; hence the extinction shown in the figures cannot be used directly to compare the concentrations. This also holds for the end times of the chromatogram. These cause an perceived overlap while this is not the case. See also Figure 14 at page 29.

MDEA calibration

Ethanol retention time: 0,89 min
MDEA retention time: 7,96 min

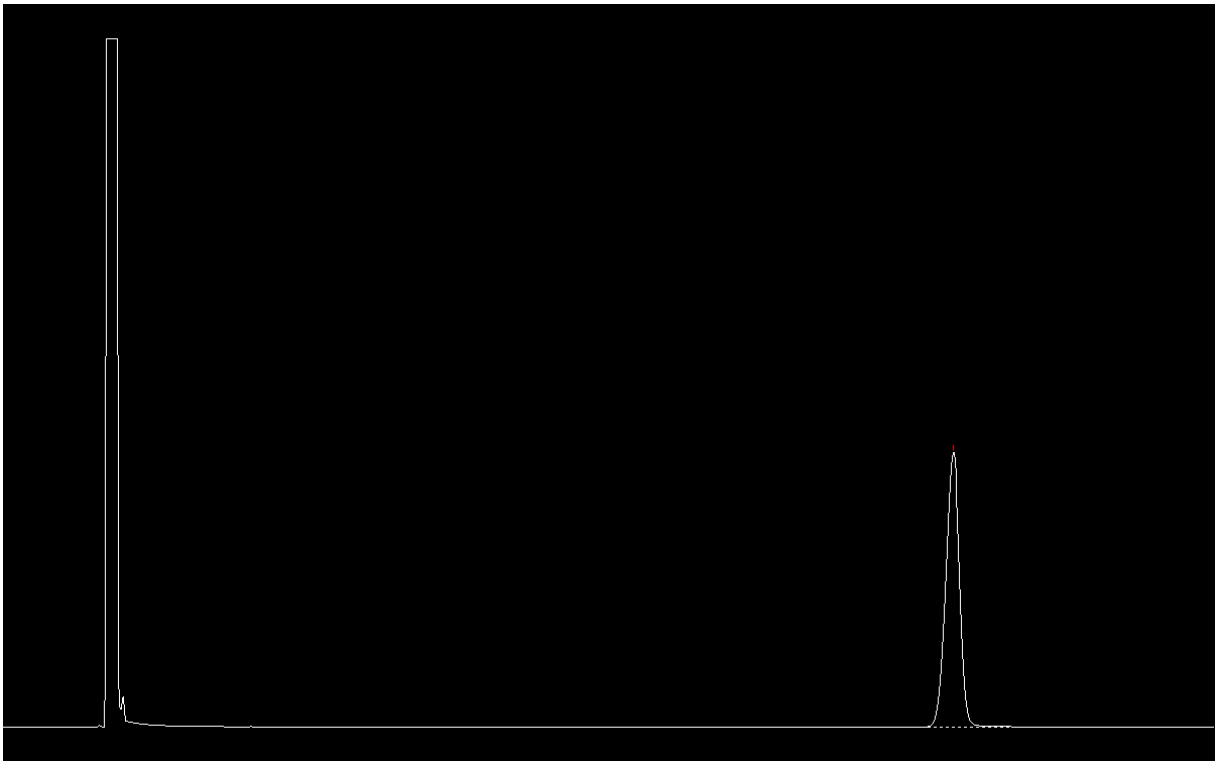

Figure 15 – Identification of the MDEA peak

Graph 19 – GC calibration for MDEA

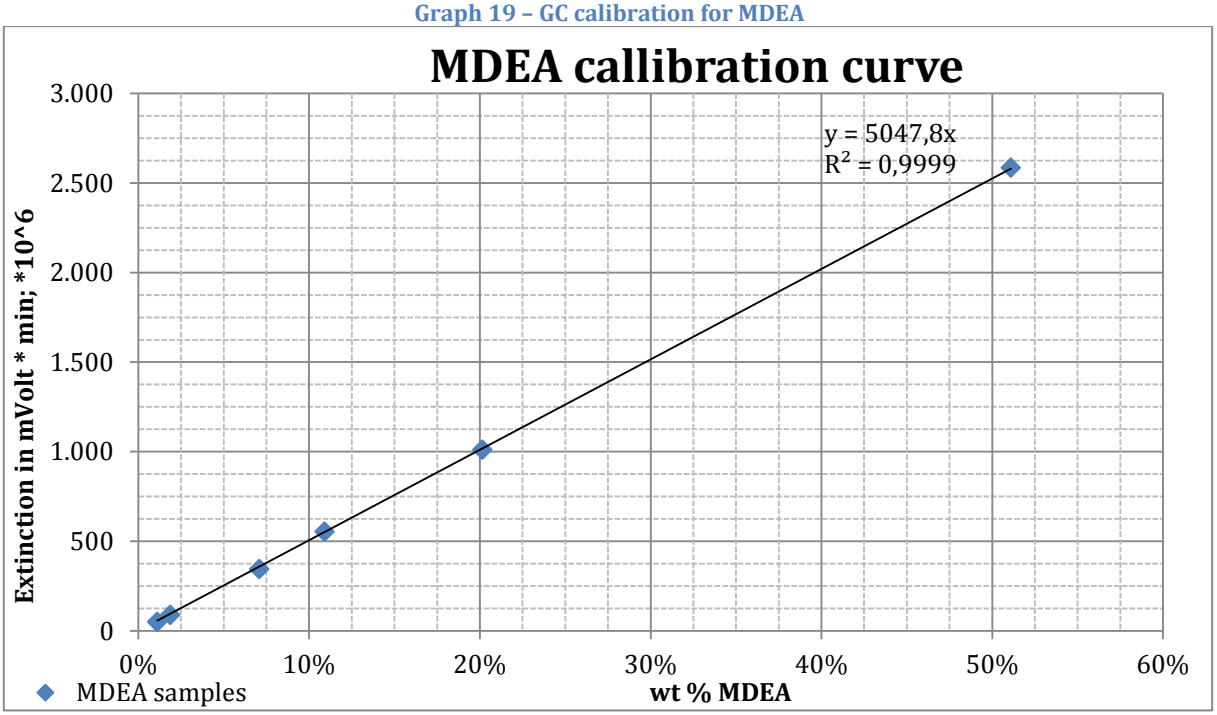

Extinction = $5.047.761.903x$; with x in wt%

AEP calibration

Ethanol retention time: 0,89 min
AEP retention time: 10,83 min

Figure 16 – Identification of the AEP peak

Graph 20 – GC calibration curve for AEP

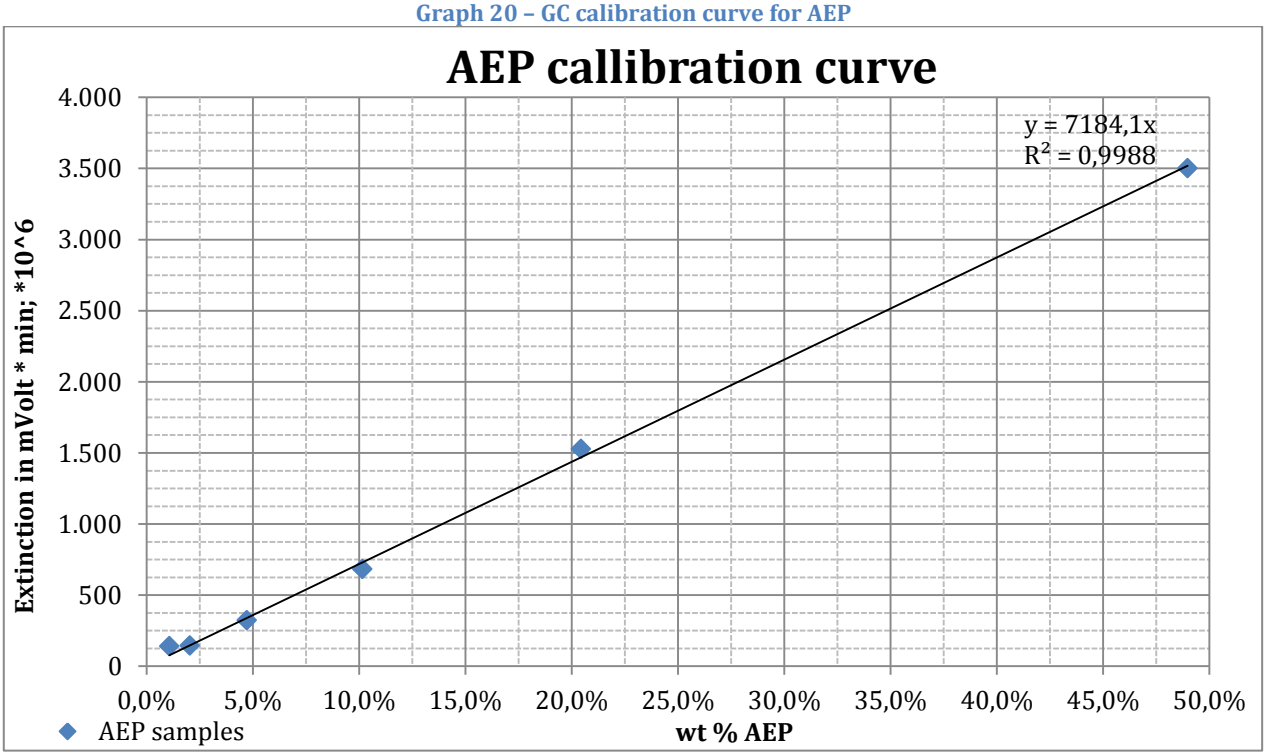

Extinction = 7.184.081.234x; with x in wt%

Sulfolane calibration

Ethanol retention time: 0,89 sec
Sulfolane retention time: 12,07 sec

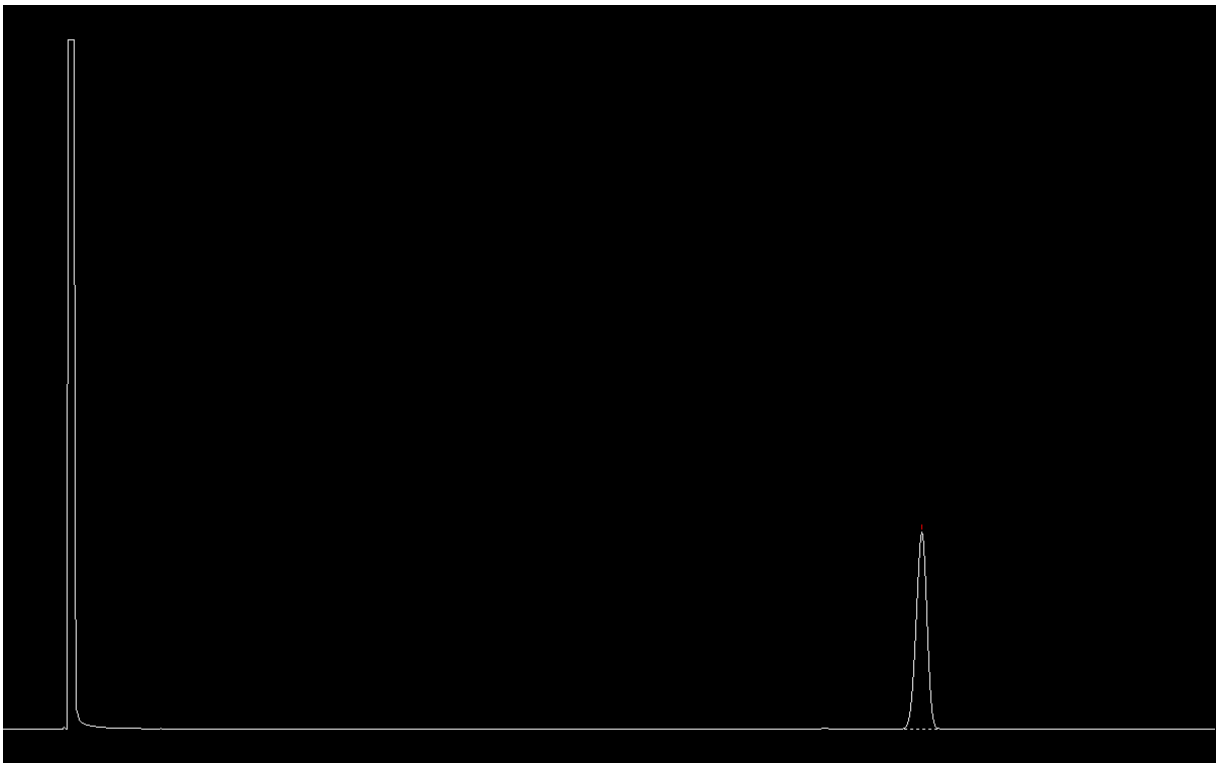

Figure 17 – Identification of the sulfolane peak

Graph 21 – GC calibration curve for sulfolane

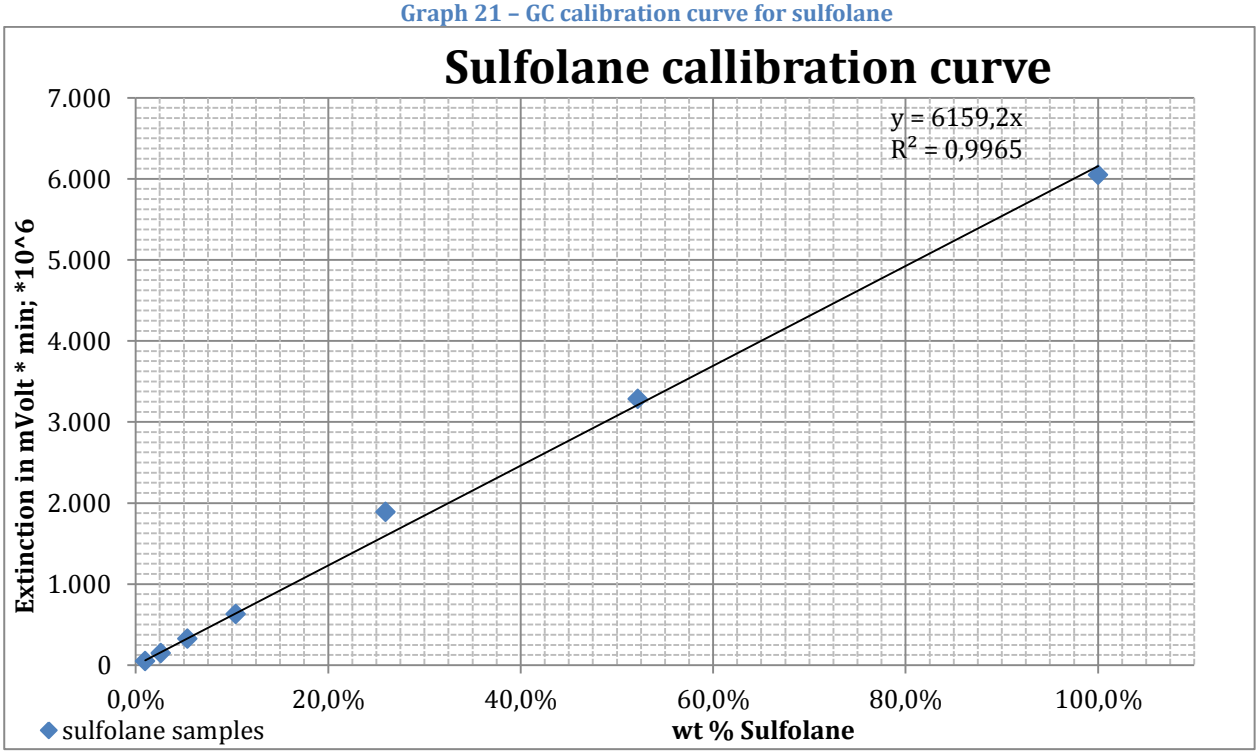

Extinction = 6.459.195.864x; with x in wt%

Appendix C – validation of the GC with a known blend

The calibration curves as presented in appendix C have been validated by using a blend of known composition. The results of this validation can be seen in the table below (Table 17):

Table 17 - Validation of the GC

Components	According to analytical balance (%)	According to GC (%)	Difference (%)
MDEA	30,0	31,2	1,2
AEP	10,5	10,7	0,2
Sulfolane	34,7	28,1	6,6

Appendix D – screening experiments 1 – 6

Experiments 1 – 6. The brown colour is due to the absorption of CO_2 by the chemical solvent.

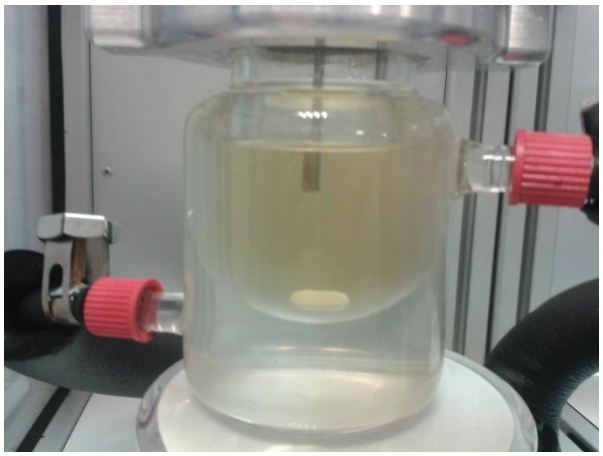

Figure 18 - AEP, MDEA & TDG (experiment 1)

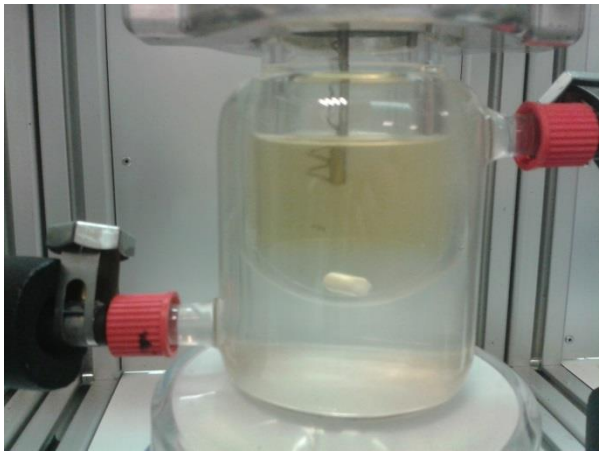

Figure 19 - AEP, MDEA & Sulfolane (experiment 2)

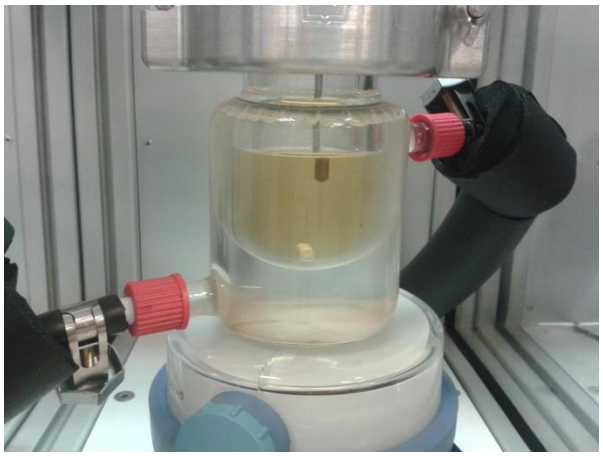

Figure 20 - AEP, MDEA & TDG (experiment 3)

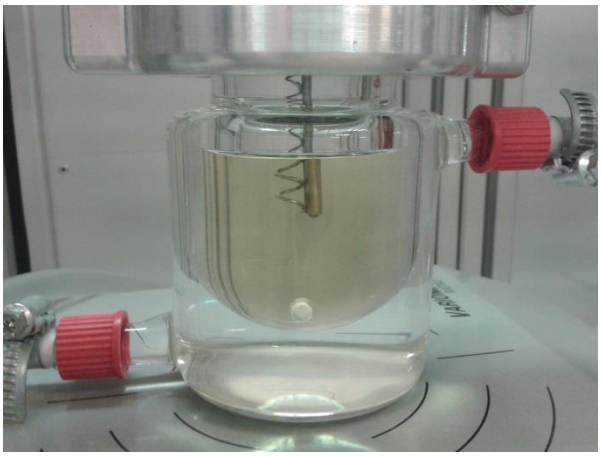

Figure 21 - AEP, AMP & TDG (experiment 4)

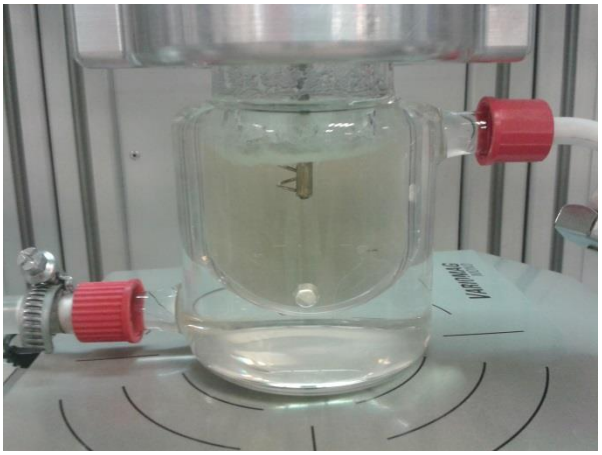

Figure 22 - AEP, AMP & Sulfolane (experiment 5)

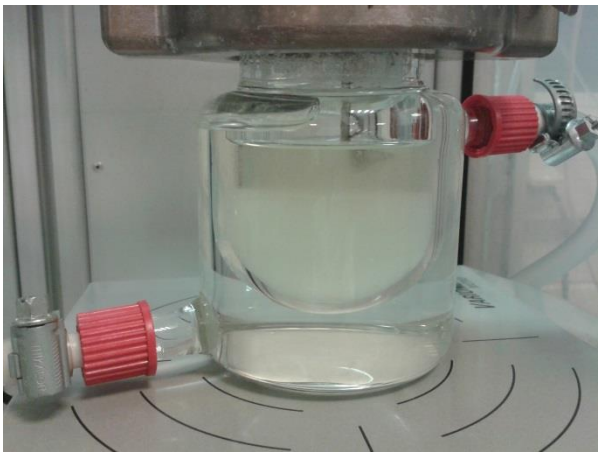

Figure 23 - AEP, AMP & TDG (experiment 6)

Appendix E – screening experiments 8 – 13

Experiments 8 – 13. The brown colour is due to the absorption of CO_2 by the chemical solvent.

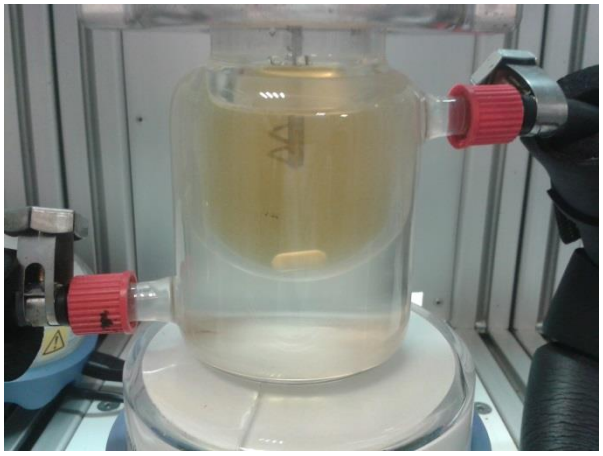

Figure 24 - AEP, MCA & sulfolane (experiment 8)

Figure 25 - MEA, AMP & sulfolane (experiment 9)

Figure 26 - MEA, MDEA & sulfolane (experiment 10)

Figure 27 - DEA, AMP & sulfolane (experiment 11)

Figure 28 - DEA, MDEA & sulfolane (experiment 12)

Appendix F – FTIR calibration for the light phase

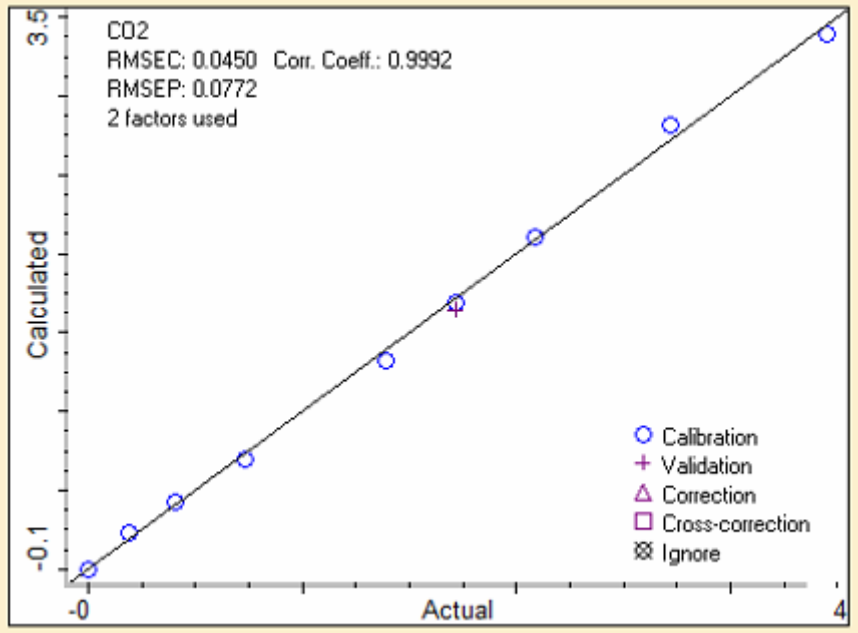

Figure 29 – Calibration and validation curve to determine the CO_2 concentration in the light phase. The unit of both axis is mole L^{-1}.

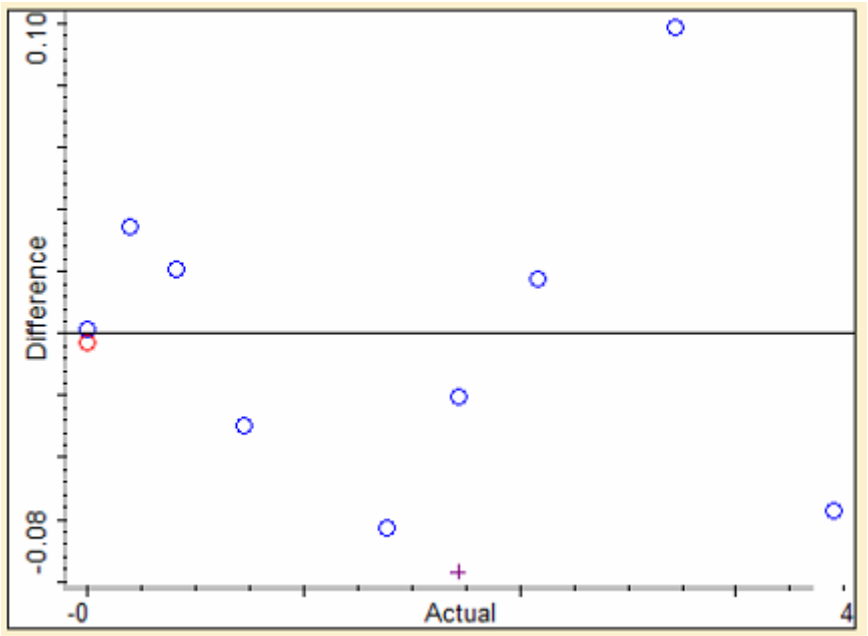

Figure 30 – Deviation between the known concentration in the samples and the calculated calibration line. Both axis show the result in mole L -1.

Appendix G – VLE run results

Original run

							AEP		MDEA		Sulfolane	
Sample	Pressure (kPa A)	phase	ethanol	sample	dillution	GC no	GC (mVolt * min)	Sample (%)	GC (mVolt * min)	Sample (%)	GC (mVolt * min)	Sample (%)
A1	93,4	light	1,3026	0,0348	38,4	batch2_04	20.165.390	10,79%	41.883.280	31,89%	43.492.620	25,88%
B1	93,4	heavy	1,4226	0,0186	77,5	108		0,00%	5.986.366	9,19%	81.172.260	97,37%
A2	120,1	light	1,3807	0,0394	36,0	batch2_04	17.979.090	9,02%	38.186.320	27,27%	50.690.190	28,29%
B2	120,1	heavy	1,3793	0,0163	85,6	110		0,00%	4.552.053	7,72%	72.114.980	95,59%
A3	145,7	light	1,3317	0,0172	78,4	111	10.630.180	11,60%	20.621.940	32,04%	14.799.000	17,97%
B3	145,7	heavy	1,4050	0,0367	39,3	112	120.325	0,07%	6.469.051	5,03%	131.671.700	80,08%
A4	196,6	light	1,2185	0,0164	75,3	113	11.053.390	11,59%	21.455.610	32,01%	12.782.950	14,90%
B4	196,6	heavy	1,4420	0,0193	75,7	114		0,00%	3.020.122	4,53%	79.546.870	93,25%
A5	306,4	light	1,4468	0,0469	31,8	116	23.763.430	10,53%	49.224.770	31,06%	30.218.240	14,90%
B5	306,4	heavy	1,3301	0,0183	73,7	121		0,00%	1.908.957	2,79%	89.406.460	101,99%
A6	442,6	light	1,4027	0,0563	25,9	119	28.765.800	10,38%	59.299.280	30,44%	34.079.300	13,67%
B6	442,6	heavy	1,4406	0,0186	78,5	120		0,00%	1.805.285	2,81%	80.243.180	97,46%
A7	458,5	light	1,2855	0,0380	34,8	batch2_04	22.818.250	11,06%	48.144.220	33,22%	24.853.660	13,40%
B7	458,5	heavy	1,5064	0,0172	88,6	126		0,00%	2.608.011	4,58%	68.333.540	93,71%
A8	708,7	light	1,2737	0,0316	41,3	batch2_01	18174410	10,45%	36.455.340	29,83%	19495580	12,47%
B8	708,7	heavy	1,3829	0,0164	85,3	batch2_020		0,00%	1108733	1,87%	66404280	87,72%
A9	1086,2	light	1,3355	0,0189	71,7	batch2_02	9348630	9,33%	19993740	28,38%	13272630	14,73%
B9	1086,2	heavy	1,4091	0,0180	79,3	batch2_022		0,00%	931957	1,46%	89070300	109,33%
A10	1489,2	light	1,3161	0,0216	61,9	batch2_02	13203980	11,38%	27867780	34,19%	15555850	14,91%
B10	1489,2	heavy	1,3656	0,0185	74,8	batch2_02	71525	0,07%	686921	1,02%	81987130	94,96%

Original run – continued

	Sulfolane		H2O		CO2 loading (mol/L)		Density		Density		
Sample (continued)	GC (mVolt * min)	Sample (%)	ppm (Karl Fischer)	Sample (%)	FTIR	accuracy	gr	gr / ml	gr	gr / ml	average
A1	43.492.620	25,88%			1,74	0,168	0,2968	1,1872	0,2939	1,1756	1,1814
B1	81.172.260	97,37%	5.853	45,35%			0,3092	1,2368	0,3076	1,2304	1,2336
A2	50.690.190	28,29%			2,67	0,112	0,3001	2,000667	0,295	1,966667	1,983667
B2	72.114.980	95,59%	5.043	43,18%			0,0624	1,248	0,0623	1,246	1,247
A3	14.799.000	17,97%	7.690	60,31%	2,29	0,145	0,2957	1,1828	0,2954	1,1816	1,1822
B3	131.671.700	80,08%	6.198	24,35%			0,3114	1,2456	0,3111	1,2444	1,245
A4	12.782.950	14,90%	8.189	61,66%	2,92	0,092	0,303	1,212	0,3009	1,2036	1,2078
B4	79.546.870	93,25%	5.493	41,59%			0,3113	1,2452	0,3106	1,2424	1,2438
A5	30.218.240	14,90%	14.330	45,64%	3,4	0,09	0,3065	1,226	0,3031	1,2124	1,2192
B5	89.406.460	101,99%	6.099	44,94%			31,66%	1,2664	0,3143	1,2572	1,2618
A6	34.079.300	13,67%	13.996	36,27%	3,52	0,094	0,3025	1,21	0,3015	1,206	1,208
B6	80.243.180	97,46%	8.247	64,70%			31,44%	1,2576	0,3131	1,2524	1,255
A7	24.853.660	13,40%	9.719	33,85%	3,41	0,09	0,3063	1,2252	0,3004	1,2016	1,2134
B7	68.333.540	93,71%	6.322	56,00%			31,05%	1,242	0,3092	1,2368	1,2394
A8	19495580	12,47%	8.556	35,34%	3,58	0,112	0,3079	1,2316	0,3052	1,2208	1,2262
B8	66404280	87,72%	1.885	16,08%			0,3144	1,2576	0,3135	1,254	1,2558
A9	13272630	14,73%	5.390	38,63%	3,33	0,09	0,3025	1,21	0,2905	1,162	1,186
B9	89070300	109,33%	4.465	35,40%							
A10	15555850	14,91%	10.134	62,76%	3,98	0,167	0,1835	1,223333	0,1862	1,241333	1,232333
B10	81987130	94,96%	5.836	43,66%			0,2496	1,248	0,2468	1,234	1,241

Duplo run

							AEP		MDEA		Sulfolane	
Sample	Pressure (kPa)	phase	ethanol	sample	dillution	GC no	GC (mVolt * min)	Sample (%)	GC (mVolt * min)	Sample (%)	GC (mVolt * min)	Sample (%)
C1	99,6	light	1,2974	0,0148	88,7	batch2_040	9.492.947	11,72%	18.899.500	33,20%	22.090.180	30,32%
D1	99,6	heavy	1,5550	0,0359	44,3	Batch2_011	0	0,00%	11.372.550	9,98%	129.341.000	88,74%
C2	126,5	light	1,4646	0,0609	25,0	129	33.220.310	11,58%	65.909.040	32,71%	45.692.280	17,72%
D2	126,5	heavy	1,2778	0,0299	43,7	batch2_042	269.137	0,16%	6.605.636	5,72%	120.549.400	81,63%
C3	157,3	light	1,4149	0,0248	58,1	131	13.451.010	10,87%	26.903.610	30,94%	17.124.540	15,39%
D3	157,3	heavy	1,5128	0,0359	43,1	Batch2_014	209.524	0,13%	6.607.010	5,65%	126.836.600	84,71%
C4	198,5	light	1,4813	0,0313	48,3	133	15.633.630	10,52%	31.676.530	30,33%	21.394.250	16,01%
D4	198,5	heavy	1,5293	0,0209	74,2	Batch2_015		0,00%	3.176.249	4,67%	85.478.840	98,16%
C5	290,7	light	1,4492	0,0439	34,0	135	20.670.110	9,79%	43.824.360	29,53%	35.948.090	18,93%
D5	290,7	heavy	1,4818	0,0343	44,2	Batch2_031		0,00%	3.379.088	2,96%	123.293.500	84,37%
C6	412,2	light	1,4311	0,0386	38,1	137	21.152.180	11,21%	43.544.200	32,85%	25.659.540	15,13%
D6	412,2	heavy	1,4300	0,0352	41,6	Batch2_032		0,00%	3.536.578	2,92%	138.802.500	89,45%
C7	496,3	light	1,5665	0,0500	32,3	143	23.475.210	10,56%	48.828.120	31,27%	30.103.330	15,07%
D7	496,3	heavy	1,5600	0,0380	42,1	Batch2_011		0,00%	2.946.332	2,45%	148.450.200	96,65%
C8	471,6	light	1,3133	0,0114	116,2	batch2_041	7.903.132	12,78%	15.412.920	35,48%	8.767.081	15,77%
D8	471,6	heavy	1,3392	0,0188	72,2	Batch2_035		0,00%	1.517.341	2,17%	84.821.530	94,86%
C9	843,2	light	1,2922	0,0186	70,5	Batch2_036	11.721.140	11,50%	23.268.830	32,49%	11.661.130	12,72%
D9	843,2	heavy	1,3265	0,0159	84,4	batch2_043			1.168.861	1,96%	79.462.500	103,86%
C10	1425,4	light	1,3549	0,0166	82,6	Batch2_038	10.208.230	11,74%	20.574.780	33,68%	9.410.835	12,04%
D10	1425,4	heavy	1,3567	0,0170	80,8	Batch2_039		0,00%	1.047.434	1,68%	73.306.340	91,71%

Duplo run – continued

	H2O		CO2 loading	Density		Density		
Sample	ppm (Karl Fischer)	Sample (%)	FTIR (mol / L)	gr	gr / ml	gr	gr / ml	average
C1	12.719	49,67%	1.72	0,0572	1,144	0,0549	1,098	1,121
D1	8.347	36,99%		0,1227	1,227	0,1221	1,221	1,224
C2	10.260	25,70%	2.85	0,5786	1,1572	0,577	1,154	1,1556
D2	3.112	20,88%		0,6185	1,237	0,6154	1,2308	1,2339
C3	5.656	32,83%	1.71	0,5867	1,1734	0,5754	1,1508	1,1621
D3	2.410	10,40%		0,6225	1,245	0,6197	1,2394	1,2422
C4	6.479	31,31%	3.1	0,5824	1,1648	0,5936	1,1872	1,176
D4	1.537	11,40%		0,6225	1,245	0,621	1,242	1,2435
C5	8.479	28,84%	3.3	0,3002	1,2008	0,2973	1,1892	1,195
D5	2.163	9,56%		31,37%	1,2548	0,3121	1,2484	1,2516
C6	8.461	32,22%	3.36	0,3016	1,2064	0,2951	1,1804	1,1934
D6	2.345	9,76%		31,33%	1,2532	0,3104	1,2416	1,2474
C7	10.191	32,95%	3.22	0,3002	1,2008	0,2968	1,1872	1,194
D7	2.370	9,97%		0,2505	1,2525	0,2495	1,2475	1,25
C8	5.069	50,52%	3.35	0,2383	1,1915	0,2339	1,1695	1,1805
D8	1.673	12,08%		0,3151	1,2604	0,3136	1,2544	1,2574
C9	5.362	37,79%	3.88	0,1243	1,243	0,1195	1,195	1,219
D9	1.775	17,38%		0,2994	1,1976	0,3016	1,2064	1,202
C10	4.829	39,90%	4.04	0,2994	1,1976	0,3016	1,2064	1,202
D10	1.707	13,79%		0,3124	1,2496	0,3121	1,2484	1,249

Appendix H – light phase loading curve

The graph shown in this appendix is the same as the graph as graph XX in paragraph YY.

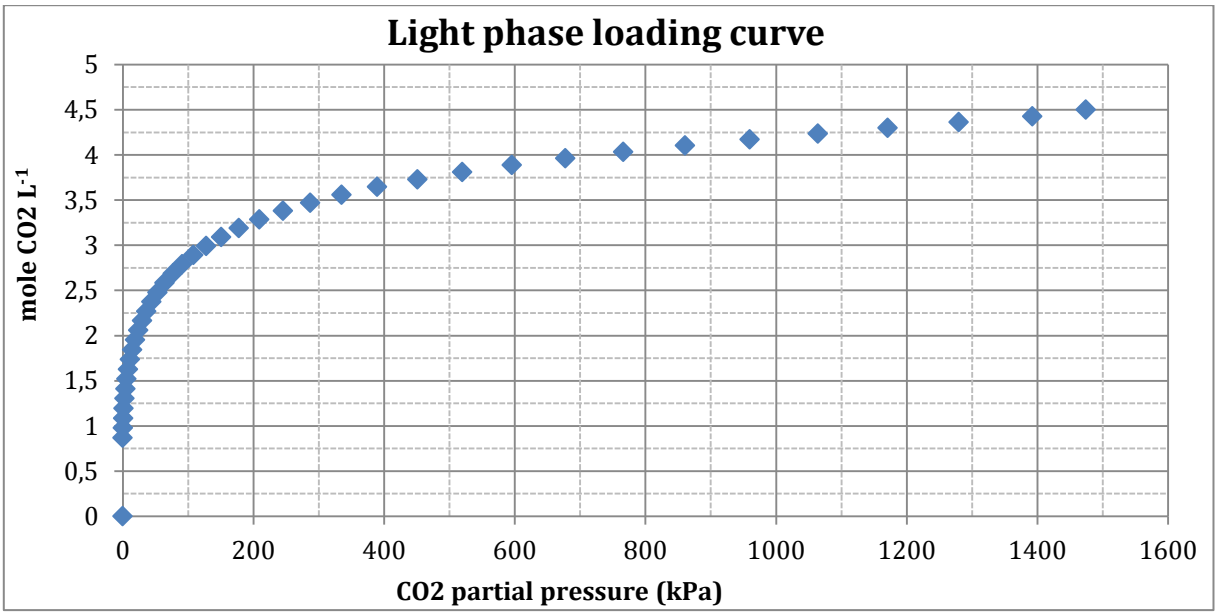

Appendix I – calculating the heat of absorption

40 = > 80 0C								
loading	P1	P2	T1	T2	ln(P2/P1)	(1/T2)-(1/	R	delta H (kJ/mol)
0,154	2,9684	0,1040	313	353	-3,35139	-0,00036	8,314	77,0
0,256	3,3182	1,1178	313	353	-1,08805	-0,00036	8,314	25,0
0,408	3,6904	4,3600	313	353	0,166732	-0,00036	8,314	-3,8
0,509	3,9980	7,4980	313	353	0,628853	-0,00036	8,314	-14,4
0,608	4,3333	12,2888	313	353	1,042355	-0,00036	8,314	-23,9
0,708	4,6983	18,4304	313	353	1,366797	-0,00036	8,314	-31,4
0,806	5,4440	27,7774	313	353	1,629703	-0,00036	8,314	-37,4
0,903	6,3497	40,2105	313	353	1,84572	-0,00036	8,314	-42,4
1,045	8,3367	65,5747	313	353	2,062523	-0,00036	8,314	-47,4
1,139	10,1389	87,8487	313	353	2,159234	-0,00036	8,314	-49,6
1,231	12,4462	115,6510	313	353	2,229162	-0,00036	8,314	-51,2
1,318	15,2252	156,0015	313	353	2,326915	-0,00036	8,314	-53,4
1,407	18,7146	189,0477	313	353	2,312695	-0,00036	8,314	-53,1
1,537	25,1130	251,7058	313	353	2,304875	-0,00036	8,314	-52,9
1,701	35,2589	363,0322	313	353	2,331772	-0,00036	8,314	-53,5

40 => 120 0C								
loading	P1	P2	T1	T2	ln(P2/P1)	(1/T2)-(1/	R	delta H
0,095	2,5511	15,4528	313	393	1,801262	-0,00065	8,314	-23,0
0,186	3,0892	34,6561	313	393	2,417575	-0,00065	8,314	-30,9
0,279	3,3794	52,6926	313	393	2,746783	-0,00065	8,314	-35,1
0,366	3,6006	82,1037	313	393	3,126873	-0,00065	8,314	-40,0
0,452	3,8111	114,9799	313	393	3,406831	-0,00065	8,314	-43,6
0,534	4,0767	156,5066	313	393	3,647808	-0,00065	8,314	-46,6
0,614	4,3364	201,2021	313	393	3,837269	-0,00065	8,314	-49,1
0,689	4,6300	255,8435	313	393	4,012009	-0,00065	8,314	-51,3

80 => 120 0C								
loading	P1	P2	T1	T2	ln(P2/P1)	d(1/T)	R	delta H
0,186	1,1627	34,6560	313	393	-3,39473	0,000650	8,314	-43,4
0,279	1,3050	52,6926	313	393	-3,69828	0,000650	8,314	-47,3
0,366	1,4224	82,1040	313	393	-4,05561	0,000650	8,314	-51,8
0,452	1,4966	114,9799	313	393	-4,34159	0,000650	8,314	-55,5
0,534	1,5310	156,5066	313	393	-4,62719	0,000650	8,314	-59,2
0,614	1,7431	201,2021	313	393	-4,74867	0,000650	8,314	-60,7
0,689	3,7024	255,8435	313	393	-4,23558	0,000650	8,314	-54,1

							average	-44,5